Robotics and Computer–Integrated Manufacturing 89 (2024) 102758

Contents lists available at ScienceDirect

Robotics and Computer-Integrated Manufacturing

journal homepage: www.elsevier.com/locate/rcim

Review

End-of-life electric vehicle battery disassembly enabled by intelligent and human-robot collaboration technologies: A review

Weidong Li [a,*], Yiqun Peng [b,c], Yu Zhu [a], Duc Truong Pham [c], A.Y.C. Nee [d], S.K. Ong [d,*]

[a] School of Mechanical Engineering, University of Shanghai for Science and Technology, PR China
[b] School of Transportation and Logistics Engineering, Wuhan University of Technology, PR China
[c] School of Mechanical Engineering, University of Birmingham, UK
[d] Mechanical Engineering Department, National University of Singapore, Singapore

ARTICLE INFO

Keywords:
Electric vehicles
Lithium-ion batteries
Human-robot collaboration
Disassembly
Echelon utilisation
Circular economies

ABSTRACT

Electric vehicles (EVs) have been experiencing radical growth to embrace the ambitious targets of decarbonisation and circular economies. The trend has led to a significant surge in the number of lithium-ion batteries (LIBs) that will soon reach the end-of-life (EoL) stage. Given that landfilling EoL EV LIBs generates substantially negative impacts on the environment, it is imperative to develop economically and ecologically sound LIB recycling solutions. This survey aims to provide a systematic update on the latest development of disassembly technology for EoL LIBs, which is a critical enabler for EV LIB recycling. First, based on a detailed analysis of major challenges incurred by large-scale EoL LIBs, two technical pillars to uphold LIB disassembly technology, i.e., artificial intelligence and human-robot collaboration (HRC), are pinpointed. Furthermore, state-of-the-art studies are analysed according to three categories, namely, LIB knowledge representation for disassembly, HRC-based LIB disassembly planning, and HRC-based LIB disassembly operations. Benchmarks are conducted on the relevant research under each category to summarise their major characteristics, pros and cons. Finally, discussions are made, and promising prospects are highlighted in a bid to inspire researchers and practitioners to explore further development of methodologies and technologies to progress towards the sustainable processing of EoL LIBs.

1. Introduction

To achieve the ambitious targets of decarbonisation, many countries have set mandates to eventually end all sales of new internal combustion engine vehicles by 2030 or 2040 [1]. In accordance with this trend, the global fleet of electric vehicles (EVs) has been experiencing radical growth. Based on the statistics of the World Economic Forum, as of 2021, there were over 16.5 million EVs worldwide. It is estimated that annual sales of EVs will increase 18-fold by 2030 [2]. The proliferation of EVs on the road is expected to lead to an exponential surge in the number of batteries that will reach the end-of-life stage in the coming decades. There are four primary types of batteries used in EVs, namely, lead acid, nickel metal hydride, lithium-ion, and sodium nickel chloride [3]. amongst them, lithium-ion batteries (LIBs), which were first introduced by Sony in its digital video cameras in 1991, have been recognised as the most promising energy solution for powering EVs. The advantages of LIBs include good energy density, long life, high efficiency charging/discharging, lightweight, and almost zero memory effect [3]. The average lifespan of LIBs is approximately 8–10 years [4]. A LIB will be considered to reach the end of its service life once the battery performance, based on the state of charge (SOC), the state of health (SOH), and/or the state of function (SOF), reflects an irreversible degradation compared to its design specification or ideal status [5]. Currently, more than 95% of EoL LIBs are landfilled or illicitly processed each year, and only a small proportion of the batteries are either repurposed for echelon utilisation or handled through shredding and comminution for material reclamation and recovery [6]. EoL LIBs contain flammable electrolytes, toxic substances, volatile organics, and carcinogenic electrolyte additives. The current practice has caused serious resource waste of scale and substantially negative impacts on the environment [7,8].

Recycling LIBs economically and sustainably has been a hot topic. More than 50% of the overall value of an EV comes from its batteries. EoL LIBs contain valuable parts and expensive and scarce metals (e.g., lithium (Li), cobalt (Co), manganese (Mn), and nickel (Ni)). They have

* Corresponding authors.
E-mail addresses: weidongli@usst.edu.cn (W. Li), mpeongsk@nus.edu.sg (S.K. Ong).

https://doi.org/10.1016/j.rcim.2024.102758
Received 18 December 2023; Received in revised form 30 January 2024; Accepted 6 March 2024
Available online 15 March 2024
0736-5845/© 2024 Elsevier Ltd. All rights reserved.

been widely regarded as "urban mines" and have ushered in some important opportunities. Battery recyclability is a key topic in the European Battery 2030+ initiative [9]. The European Commission proposed a mandatory regulation that specified recycled contents from recycled LIBs need to be used to replenish new battery production. It requires that by 2035, new LIB production for EVs must contain at least 20%, 12%, and 10% recycled Co, Ni, and Li, respectively [10]. Meanwhile, effective recycling of obsolete LIBs can mitigate potential damage to the environment and promote ecological advantages [11]. In recent years, sustainable recycling technologies for LIBs have been actively explored. The hierarchy mainly includes echelon utilisation, remanufacture, and material recovery. After checking and eliminating safety risks, echelon utilisation can repurpose and regroup spent LIBs with considerable remaining capacities into commercial or specially purposed energy storage systems [12]. Remanufacturing aims to replace defective modules to restore LIBs and provide a product warranty that is equal to or close to that of a newly manufactured equivalent [13]. For material recovery, valuable and scarce materials contained in LIBs can be reclaimed and recirculated back into LIB production cycles.

As a preliminary step but also a bottleneck in the above LIB recycling processes, disassembly is used to dismantle high-value parts from LIBs to facilitate downstream recycling activities. Disassembly of parts of interest at the LIB pack-, module-, and cell-level can support metallurgical, chemical, and physical separation processes for material reclamation in purer states [14–16]. With effective disassembly, it has been proven that a high recovery yield of over 80% of the total LIB mass can be produced. Therefore, disassembly is regarded as a must-have process rather than an optional solution [17]. Presently, manual disassembly by skilled human operators has been predominantly adopted in industries. It is tedious and difficult to scale up economically due to high labour costs and low efficiency. Due to the tremendous amount of spent or soon-to-be spent LIBs, it is an inevitable trend to develop automated disassembly technologies [18]. In recent years, industrial robots have been explored to some extent to carry out unfastening, unscrewing, disconnecting, grabbing, and other repetitive jobs to support LIB disassembly automation. The use of industrial robots can reduce costs and improve efficiency, potentially making LIB recycling economically viable. On the other hand, some significant challenges and barriers to robotic LIB disassembly automation exist. Industrial robots are characterised by high repeatability, but they lack the versatility to effectively handle sophistication and uncertainties occurring during LIB disassembly, such as highly diverse LIB models, deformed and soft parts, corrosive fixtures, and complex adhesive bonding in LIB assembly. Developing robotic systems that can be used for a variety of products and handle process uncertainties remains a major challenge at the frontier of robotics and artificial intelligence research [11]. Currently, synergetic robotic automation and human-based dexterity are desirable because they can provide a flexible solution to meet the multifaceted requirements of EoL LIB disassembly. Thus, human-robot collaboration (HRC)-based disassembly is promising for providing pivotal solutions to enable flexible LIB remanufacturing when the human safety is ensured [19]. To the best of the authors' knowledge, the first trial using HRC to disassemble LIBs was conducted in 2018 by Gerbers et al. [20]. Moreover, there are various decision-making processes throughout LIB disassembly. Rapidly progressing artificial intelligence (AI) technologies, such as machine learning, deep learning, and reinforcement learning (RL), can be introduced to enhance HRC by realising machine intelligence. For instance, HRC-based disassembly activities, such as the detection of deformed and defective parts in LIBs, modelling and control of HRC during disassembly processes, HRC disassembly planning and scheduling, and robotic manipulation learning for specific LIB disassembly operations, can be optimised by using state-of-the-art intelligent strategies [21,22].

Given the significance of LIB disassembly, it is highly valuable to summarise key enablers and the latest technical advances to shed light for industries and academics to progress forward. In this survey article, a major focus is on the update of two pillars to uphold LIB disassembly, namely, AI and HRC technologies. To ensure that this survey is comprehensive, disassembly methodologies that have been developed for other products are included, and their applicability to EoL LIBs is discussed. This survey was conducted by searching for related papers in recent years using a series of terminologies related to EVs, LIBs, recycling, reuse, remanufacturing, disassembly, echelon utilisation, HRC, AI, sustainability, etc. The search was also carried out in conjunction with the interdisciplinary combinations of the above terminologies. The databases and search engines used include ScienceDirect, IEEE Xplore, Springer, Google Scholar, Web of Science, and Scopus. Literature screening focused on international journals and conference proceedings in the research fields of environment, engineering, robotics, manufacturing, and computer science. Fig. 1 shows a steady increase in related publications in the last ten years, which has been motivated by strong industrial, societal, ecological, and ethical requirements for LIB recycling topics. There are several survey papers published in this area, but most of them are concerned with material recovery processes, and very few studies summarise LIB-based disassembly technologies (see Table 1). This survey article is aimed at providing a more comprehensive summary of LIB-based disassembly technologies and the enabling AI and HRC technologies. The related research has been categorised as LIB decision-making knowledge representation for disassembly, LIB disassembly planning, and LIB disassembly operations, as shown in Fig. 2.

2. HRC-based intelligent disassembly and research issues

2.1. Typical LIB structures and configurations

Although EV LIBs vary in terms of size, shape, capacity, and weight, they share some common principles in configurations and chemistries. A typical LIB has a hierarchical structure consisting of packs, modules, and cells [11,13,26]. LIB packs are assembled within a housing cover, which consists of two parts, namely, a lower tray and an upper cover. A LIB pack is composed of a certain number of battery modules, battery management systems, cables, electrical connections, a cooling system, and insulation. Battery cells, which are bracketed in each battery module, are usually formed by four main components: anode, cathode, electrolyte, and separator. The anode and cathode are manufactured with lithium metal oxide and lithiated graphite. In the most common configuration, an anode consists of a copper foil coated with graphite, and the cathode has an aluminium foil coated with $LiNi_xCo_yMn_zO_2$. Similarly, a cathode is coated with a mixture of active cathode material, including a certain ratio of cathode material, a binder, and additives. An electrolyte is made of lithium salts and organic solvents. A separator, which segregates an anode from a cathode, is permeable and has a microporous membrane allowing lithium ions to pass through pores. Cells can usually be configured as cylindrical, prismatic, or pouch-shaped. They are different in housing material and electrode-separator compound design. The cylindrical and prismatic cells consist of a welded case (aluminium or stainless steel) in which an electrode coil is inserted. For pouch cells, the electrode stack is enclosed by a heat-sealed z-folding pouch foil, which is usually made of a polyamide-aluminium-polypropylene compound. Fig. 3 illustrates the hierarchical structure of a LIB and the echelon utilisation, disassembly, and metallurgical separation of material reclamation after the service life of the LIB in EV use is finished [11,26].

2.2. Recycling routing and disassembly requirements for EoL LIBs

Analysis of recycling routes to make a sensible choice is an essential step for processing EoL LIBs after they are removed from EVs, discharged, and stabilised. The decision-making processes are related to economic values, environmental targets, LIB conditions and capacities, health and safety factors, etc. Based on the above information, recycling and disassembly plans can be determined. Typical recycling routes for EoL LIBs are illustrated in Fig. 4.

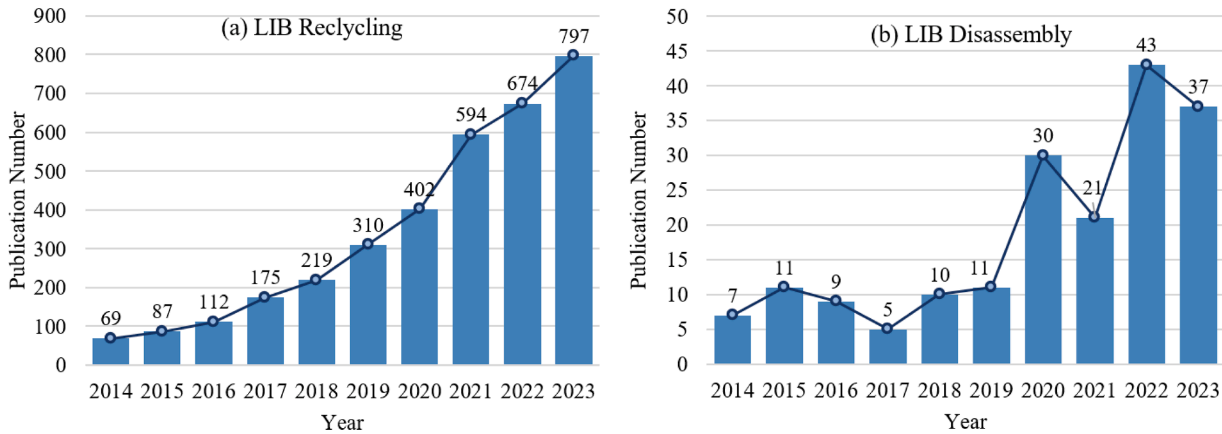

Fig. 1. Related papers in the research field reflecting the trend.

Table 1
Related surveys to summarise LIB recycling and disassembly processes.

Ref.	Research scopes	Year
Liu et al. [23]	Review of the state-of-the-art research on spent LIB recycling with emphasis on lithium recovery.	2019
Harper et al. [11]	Review of the state-of-the-art research on spent LIB recycling, including pyrometallurgy, physical materials separation, hydrometallurgy, direct recycling, and biological metals reclamation.	2019
Lai et al. [24]	Criteria, policies, regulations, costs, values, and key technologies for echelon utilisation of spent LIBs are comprehensively reviewed.	2021
Neumann et al. [25]	Regulations and initiatives for recycling LIBs are reviewed. State-of-the-art LIB recycling technologies, including pretreatment, discharging, and material recovery, are summarised. In particular, recycling technologies for specific components in LIBs are reviewed.	2022
Meng et al. [17]	Artificial intelligence/machine learning technologies that boost end-of-life LIB disassembly are reviewed.	2022
Wu et al. [4]	Disassembly technologies for end-of-life LIBs are reviewed, mainly including disassembly sequencing, manual experimental disassembly, and automatic disassembly implementation.	2023
This survey	A more comprehensive summary of LIB-based disassembly and the supporting technologies, i.e., artificial intelligence and HRC, are given. The survey is carried out according to LIB knowledge representation for disassembly, disassembly planning, and disassembly operations.	2024

EVs have stringent requirements for battery capacities [4,12]. According to current standards and practices, a LIB with 70%−80% of the initial SOH should be retired from EV use and could be reused in a second life (e.g., echelon utilisation). When the reused LIB further declines to approximately 30%−40% of the initial capacity, it could be in the stage of material-level recovery [17,24]. Briefly, the recycling routes can be classified into the following categories:

- Echelon utilisation. Module-level and pack-level echelon utilisation are commonly adopted schemes [24]. These schemes exhibit different characteristics and applicability. The former is a good echelon utilisation solution in terms of flexibility and expansibility. Less complicated disassembly operations are needed to dismantle EoL LIBs from packs to modules. The latter, which involves limited disassembly operations, demonstrates good safety and economic feasibility for building large-scale energy storage systems. However, the packs are difficult to regroup and are constrained by application scenarios due to their high diversity in shape, structure, and external features. The choice of a suitable echelon utilisation scheme depends on the capacities, conditions, safety, cost, and application scales of spent LIBs. In comparison with the above schemes, cell-level echelon utilisation is less recommended from the perspective of economy and safety [24];
- Material recovery. The major industrial LIB material recycling technologies are pyrometallurgy, hydrometallurgy, and direct recovery [4]. Biometallurgy is still under development at the lab scale [4,25,30]. The above processes have been designed for LIBs with different cell chemistries. Pyrometallurgy is more suitable for recycling batteries with high cobalt and nickel contents. After crushing, shredded materials are separated to remove passive fragments and large-sized particles. The resulting powder (called black mass) is further processed via thermal and burning treatments. Lithium and aluminium left in slags are recovered using leaching, filtering, and evaporation processes [4]. Hydrometallurgy, which enables the recovery of lithium, cobalt, manganese, and nickel, is applicable to a mixture of different cathode types. The essential process consists of leaching using a wide variety of acids or alkalis, followed by separation and refinement processes. Direct recovery can mine cathode materials by hydrothermal, froth, and sinter processes with comparatively low environmental impact. Single cathode materials are needed as input to recover high-quality materials [25].

In the above processes, disassembly is indispensable. LIBs need to be disassembled at least to the module level for echelon utilisation or pyrometallurgy and hydrometallurgy. For direct recovery, LIBs need to be disassembled further down to the level of cells and individual electrodes to achieve purer material separation and more efficient collection of active materials. Some research related to LIB disassembly levels and depths are listed in Table 2.

2.3. Major challenges and critical research topics for intelligent hrc disassembly

In recent years, some pilot robotic or HRC-based solutions for LIB disassembly have been reported [19,20,27-29,34,35]. Nevertheless, there are remarkable challenges in implementing industry-scaled HRC disassembly. The following challenges are identified and summarised in Table 3:

- Lack of LIB knowledge representation. Due to intellectual property rights (IPR) and commercial considerations by LIB developers, not all LIB digital design models are publicly available or accessible. Without the critical knowledge representation, it is difficult to decide on the disassembly operations and their sequence. Meanwhile, the original shape and condition of a LIB could change during its

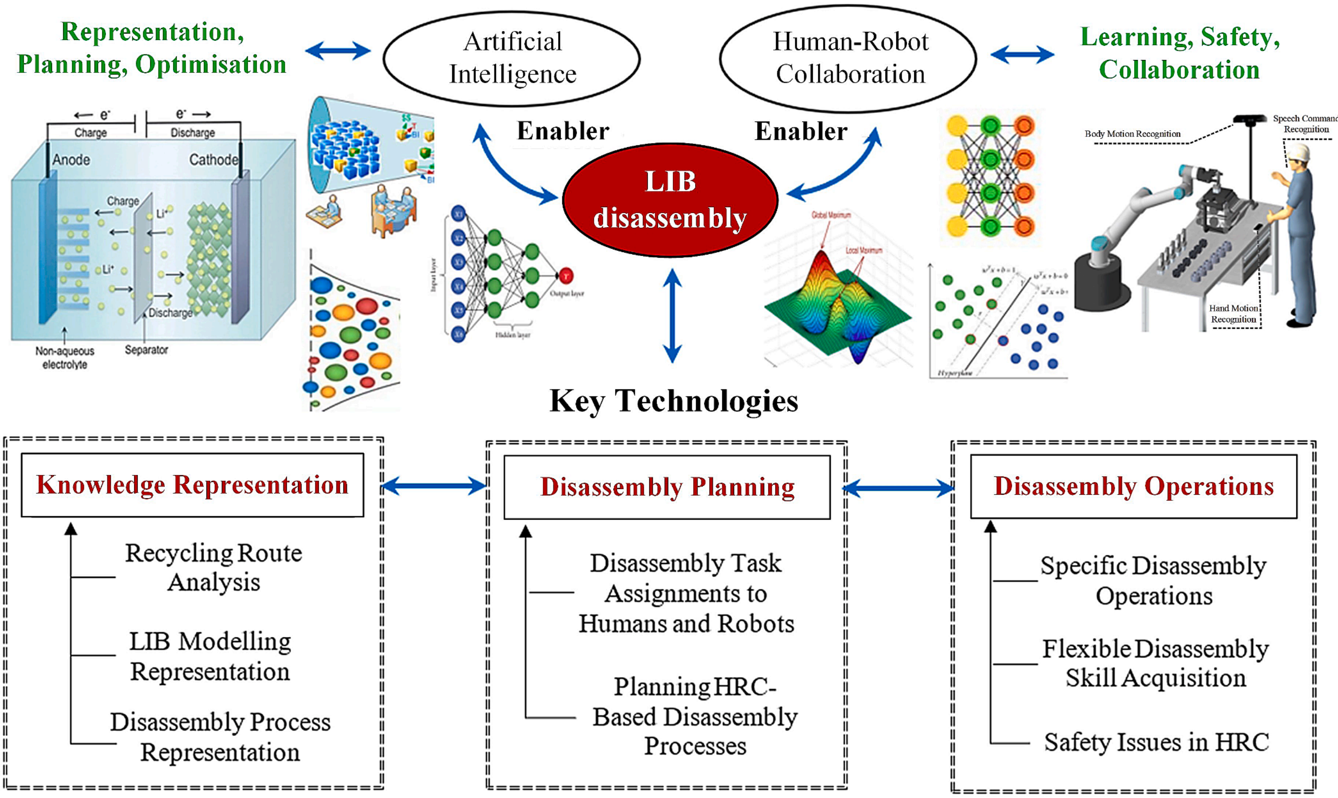

Fig. 2. Major research categories summarised in this survey.

lifecycle. Without the updated knowledge, the positioning accuracy of HRC-based disassembly will be significantly affected;

- High varieties of EoL LIB models. There are no international standards for EV LIB design [11]. EVs are usually developed based on redesigning conventional car models with only small adjustments to the models; therefore, batteries vary along with car bodies [22]. LIB varieties are exaggerated by strong demands for customised EVs, and consequently, LIBs differ not only by each car manufacturer but also by each car model [11]. These issues make HRC-based LIB disassembly processes highly customised, which necessitates intelligent decision-making processes during disassembly planning/replanning;
- Complicated conditions of EoL LIBs. A LIB pack comprises multiple modules with numerous cells connected in different configurations with various joining technologies (e.g., flexible cabling, adhesive bonding, welding). Meanwhile, due to the lack of in situ monitoring measures and lifecycle management procedures in place, it is difficult to obtain abundant historical data about LIB lifecycle utilisation. Thus, the assessment and prediction of the conditions and remaining lives of LIBs are inaccurate, which makes it challenging to plan HRC-based LIB recycling and disassembly operations;
- Human and robotic issues during LIB disassembly. A pure human-based disassembly solution for EoL LIBs faces various safety and health issues, such as electric shock, toxic gas and noxious byproduct generation, hazardous chemistry exposure, and electrolyte leakage. Barriers to the adoption of a pure robot-based disassembly solution include fastener connections that are not disassembly-friendly, parts in an unstable form and location (e.g., cables needing to be cut), difficulties in removing rusted screws and bolts, etc. Therefore, the complementary strengths of humans and robots should be optimised to establish rational joint capacities to pursue safe, flexible, and efficient disassembly processes.

The purpose of this survey is to update the state-of-the-art research on intelligent HRC technologies that address the challenges facing EoL LIB disassembly. The critical research topics to be investigated are summarised as follows (also shown in Table 3):

(1). Knowledge representation for EoL LIBs. It is essential to choose the most appropriate recycling routes for EoL LIBs from the perspective of relevant regulations, LIB-specific conditions and capabilities, economic and environmental targets, safety factors, target markets, etc. It can be facilitated by some preprocessing tasks, such as condition checking, performance testing, and used product sorting. Furthermore, geometric models of EoL LIBs and the disassembly relationships of critical parts/components/materials in the models need to be established. Thus, disassembly planning can be developed subsequently, and valuable parts and hazardous materials in LIBs can be positioned precisely during subsequent processes;

(2). HRC-based LIB disassembly task planning. Strategic and operational decisions for HRC-based LIB disassembly are determined during this stage. The decisions include the overall disassembly optimisation objective definition based on economic, environmental, and social targets, HRC task allocation based on the limits and complementary strengths of humans and robots, disassembly line balancing, scheduling and dynamic adjustments, etc.;

(3). HRC-based LIB disassembly operations. Major LIB disassembly operations are how robots locate, grip, disconnect, and separate parts. The mechanisms of different non-destructive connecting and joining configurations in LIBs suitable for robotic disassembly operations are analysed. Important topics to be surveyed include risk assessment and human safety protection measures during HRC-based disassembly, robotic disassembly operations and control via human teleoperations and demonstration-enabled learning, and human-robot iterations to carry out joint disassembly.

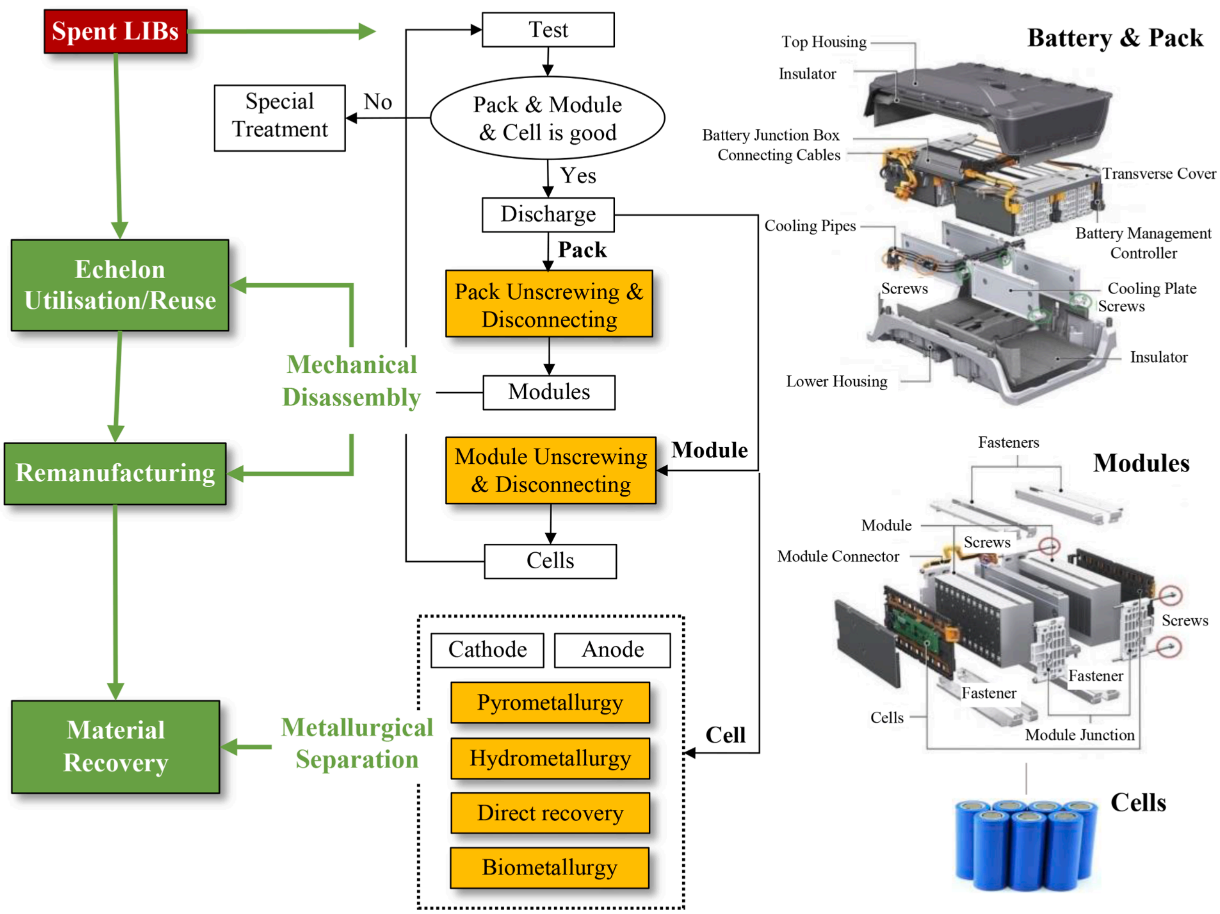

Fig. 3. Echelon utilisation, disassembly, and material reclamation processes for an EV LIB (the LIB model in the figure is from [13]).

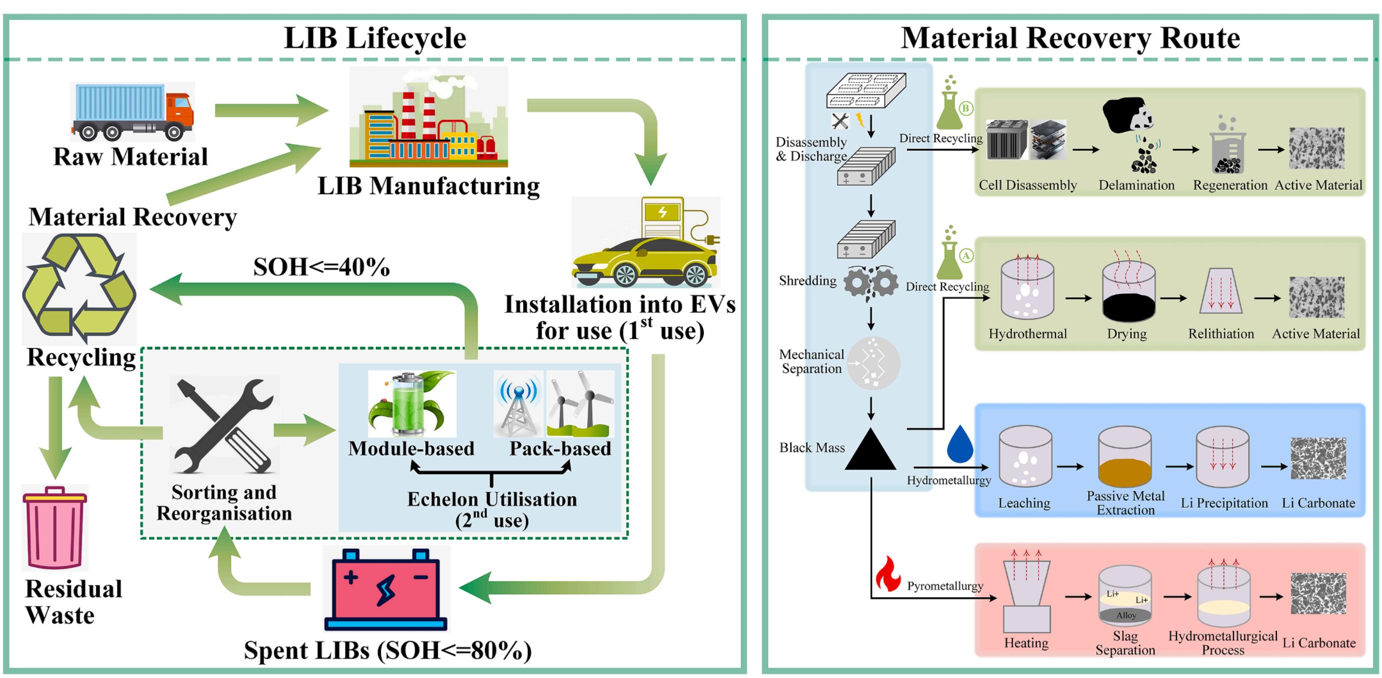

Fig. 4. The recycling route for spent LIBs [4,24].

Table 2
Spent LIB disassembly studies.

Ref.	Disassembly Automation	Intelligent Technologies	Disassembly Depths	Disassembled Batteries
Wegener et al. [27], 2015	Robot-based	Not mentioned	Pack-to-module, Module-to-cell	Audi Q5 hybrid battery
Rallo et al. [12], 2020	Manual	Not mentioned	Pack-to-module	Smart ForFour battery
Marshall et al. [31], 2020	Not mentioned	Not mentioned	Module-to-cell	1st-generation Nissan Leaf
Rastegarpanah et al. [32], 2021	Multirobot-based	Not mentioned	Pack-to-module	Not mentioned
Rosenberg et al. [33], 2022	Manual	Fuzzy logic	Pack-to-module	Batteries of a Mercedes plug-in hybrid EV
Zhou et al. [21], 2022	HRC-enabled	Stackelberg model	Pack-to-module	Not specific
Chu and Chen [34], 2023	HRC-enabled	Hybrid particle swarm optimisation and Q-learning	Pack-to-module, module-to-cell	Model S
Yuan et al. [35], 2023	HRC-enabled	Integrated fuzzy Bayesian fusion and analytical network	Pack-to-module, module-to-cell	Not specific

3. Knowledge representation and modelling for spent products (including LIBs)

Knowledge representation and modelling for EoL products are essential in supporting HRC-based disassembly planning and execution. It includes three aspects: (i) recycling route analysis for EoL products, (ii) EoL product modelling, and (iii) EoL product disassembly process modelling. The following analyses are not limited to LIBs but also include case studies for other products. The applicability of the developed methodologies to EoL LIBs will be explored.

3.1. EoL product modelling

During HRC-based disassembly, computer-aided design (CAD) models of EoL products (including LIBs) are not always obtainable. The conditions and precise shapes of parts in the products after long service could also be different from those of their original models. Computer vision systems have been developed to model spent products to support subsequent disassembly activities. Fig. 5 illustrates two scenarios of using 2D/3D data to model EoL LIBs. Table 4 presents a summary of the related research. The details of the research are elaborated next.

Data perceived by vision sensors as input to vision systems can be either 2D images that are represented in the form of RGB or 3D point clouds that are represented as a series of spatial points in cartesian coordinate systems. Modelling algorithms to process 2D images can be categorised into two types, namely, one-stage target detection algorithms and two-stage target detection algorithms. They are distinguished by how the objects in 2D images are located and classified. The former directly processes the image of an entire product and produces the 2D geometries of the product in the image. Examples of such algorithms include the widely used 'you only look once' (YOLO) algorithm and its variants [49]. The latter initially processes the image of an entire product to generate multiple distinct detection boxes (anchors). Subsequently, the position of each detection box is refined, and the type of part contained within the box is classified. Prominent representative algorithms include the regional convolutional neural network (R-CNN) and its variants, such as Fast R-CNN, Faster R-CNN, and masque R-CNN [50]. Theoretically, the R-CNN series of algorithms has a higher detection accuracy than the YOLO series of algorithms. However, this enhanced precision comes at the cost of slower processing speeds. The R-CNN series of algorithms has been successfully used to recognise smaller product parts. For instance, the positions of screws in spent mobile phones were detected using the Faster R-CNN algorithm [38]. The region proposal network of the Faster R-CNN was optimised based on the unique size ratio of screws [39]. This optimisation process reduces the generation of invalid anchors, leading to improved detection efficiency and accuracy. Zhang et al. [37] determined whether a screw was tight by using the Faster R-CNN algorithm to process the side image of the screw. The average detection accuracy reached 95.03%. masque R-CNN exhibits the ability to classify pixels in an image, thereby aiding in positioning parts. Su et al. [41] employed the masque R-CNN algorithm to analyse parts of an EoL laptop. Compared to the R-CNN series of algorithms, the YOLO series of algorithms demonstrate a faster detection speed and are therefore suitable for modelling scenarios with high real-time requirements. Brogan et al. [44] designed a Tiny-YOLO v2 system specifically for detecting cross-recessed screws. The accuracy of the three test sets reached 92.60%, 99.20%, and 98.39%, respectively, and the processing time per frame was only 0.33 s. Mangold et al. [42] employed the YOLO-v5 algorithm to locate and classify six screw heads of different sizes for a remanufactured motor. Furthermore, it is worth noting that transfer learning methods can be combined with deep learning algorithms to enhance their functions. For instance, Foo et al. [36] employed pretrained network weights from the COCO dataset to initialise the lower layer parameters of Faster R-CNN for part detection on spent LCD monitors. The transfer learning mechanism in the research effectively enhances the speed and accuracy of training by compensating for training data scarcity.

Relying solely on a 2D image provides planar data on EoL products. To enable effective application in practical settings, an additional transformation can be applied to spatial data by utilising depth information [51]. Nevertheless, this approach is hindered by variations in illumination and the lack of spatial information when only recognising 2D images. It has therefore prompted researchers to advocate the direct

Table 3
Challenges and critical research topics for spent LIB disassembly.

LIB characteristics	Health and safety issues	Joining and connections	Human issues	Robotic issues	Research issues
• Variety of LIB models • Variety of end-of-life conditions • Diversity of chemistries • Deformed and polluted parts • Model information missed	• Electric shock • Thermal runaway • Toxic gas • Hazardous chemistry • Leaked electrolyte	• Variety of connections • Deformed connections • Flexible cabling • Adhesive bonding • Permanent connections and welds	• High cost and tooling • Training • Expensive protection measures • Low efficiency	• Programming for changing conditions • Difficult access to complicated parts • Difficult operations for complicated connections	• Knowledge representation of spent LIBs • HRC task allocation • Disassembly planning optimisation • Disassembly operation optimisation

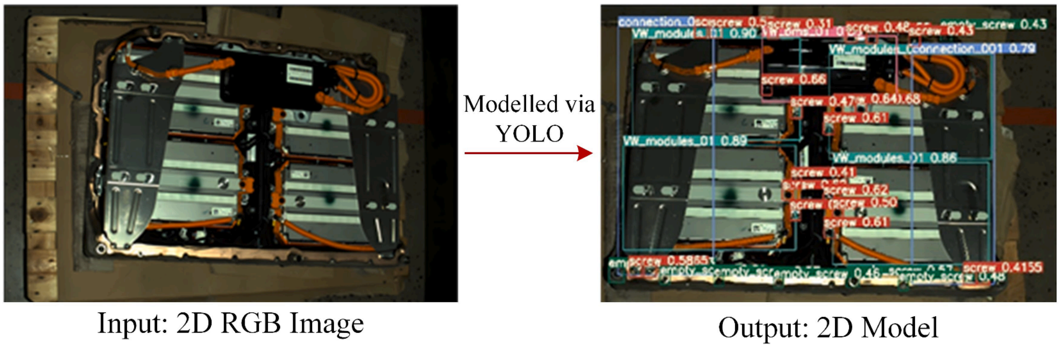

(a) Modelling for a 2D RGB image of an EV LIB.

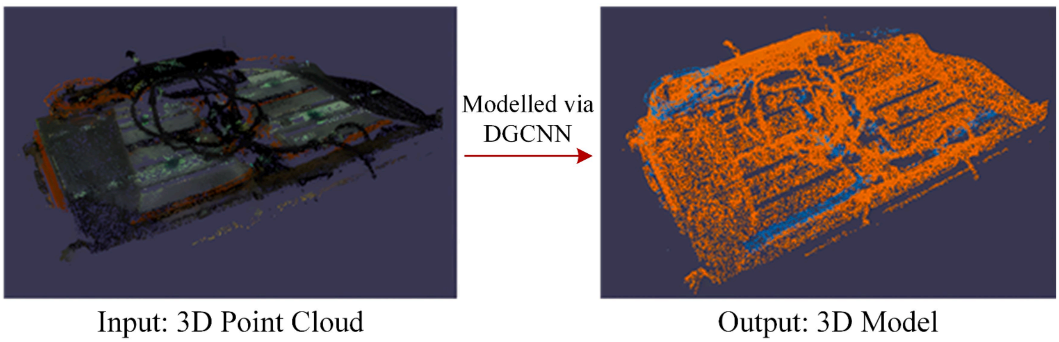

(b) Modelling for a 3D point cloud of an EV LIB.

Fig. 5. Modelling for a 2D RGB image and a 3D point cloud of EV LIBs [43,47].

Table 4
Research on establishing disassembly models.

Data	Methods	Advantages	Disadvantages	Applications
2D-RGB image	Region-proposal-based two-stage detection	• Separate steps for region selection and classification • High detection accuracy • Capable of handling multiscale and small object detection	• Slow detection speed • Complex structure • High number of samples needed for training	• Foo et al. [36]: screw modelling • Zhang et al. [37]: bolt modelling • Li et al. [38]: screw modelling • Bai et al. [39]: fastener modelling • Athanasiadis et al. [40]: WEEE modelling • Su et al. [41]: laptop part modelling
	Region-free one-stage detection	• Simple algorithmic structure • Fast detection speed	• Low detection accuracy • A large number of samples needed for algorithm training	• Mangold et al. [42]: screw modelling • Choux et al. [43]: EV LIB modelling • Brogan et al. [44]: screw modelling • Chen et al. [45]: circuit board component modelling
3D-point cloud	Point-based	• Take raw point cloud as input • High detection accuracy	• Relatively complex structural design • Difficult to label data	• Zheng et al. [46]: instance segmentation for turbochargers • Brådland et al. [47]: instance segmentation for EV LIBs • Wu et al. [48]: instance segmentation for motors
	Multi-view-based	• Relatively simple structure • Ability to be integrated with 2D processing algorithms	• Low detection speed • Difficult to label data	• Adesso et al. [52]: fastener modelling • Bilal et al. [53]: EV LIB modelling

processing of 3D point cloud data. For disassembly-related research, direct utilisation of deep learning algorithms can process 3D point cloud data, enabling more accurate instance segmentation of products. For disassembly, current deep learning algorithms for processing 3D point clouds can be generally categorised into multi-view-based approaches and point-based approaches. The multi-view-based approaches involve projecting point clouds into 2D images and then 2D convolutional networks are used for classification. For instance, Adesso et al. [52] arranged 12 cameras on a sphere containing 3D fasteners, and each fastener was described by 12 grayscale images of 244×244 pixels. Each image was processed using a VGG16 network to determine the class of fasteners by averaging the scores of the results. Bilal et al. [53] placed a LIB pack in the centre of an ellipsoidal structure, and eight cameras were arranged to acquire 2D images. Each component of the battery pack was detected using the YOLO v5 algorithm. However, the multi-view-based approaches are computationally inefficient due to the need to process multiple views. In contrast, the point-based approaches work directly on the original point clouds without any projection, so they are more efficient than the multi-view-based approaches. The PointNet network represents the earliest application of point-based approaches to processing point cloud data [54]. Zheng et al. [46] applied the PointNet network to classify each part within an EoL turbocharger from a set of point clouds. Wu et al. [48] designed a novel approach using the dynamic graph convolutional neural network (DGCNN) with the EdgeConv module. Brådland et al. [47] utilised multiple point cloud processing algorithms (including support vector machine (SVM), PointNet, DGCNN) to identify parts in EoL LIBs. Experiments indicated that DGCNN exhibited more robust accuracy and higher efficiency when processing a large amount of point cloud data. However, there are still some challenges in point cloud data processing, such as slow processing speed, sparse and uneven point clouds, and difficult labelling.

In conclusion, computer vision presents a reliable approach for representing vital information, encompassing the size, position, and part status of EoL products. While there are limited studies focusing specifically on using computer vision to model EoL EV LIBs, numerous successful application scenarios have been developed for other retired products, such as laptops, motors, and LCDs. These techniques can be readily extended to model and represent EoL EV LIBs and their parts, such as screws, housings, cables, etc. This capability effectively addresses the challenge of incomplete or imprecise CAD information available, thereby facilitating the practical implementation of LIB disassembly processes.

3.2. Disassembly process modelling

It is essential to develop models to represent disassembly processes. The developed models mainly include the AND/OR graph, the Petri Net (PN), and the matrix-based method. Table 5 presents a summary of these models.

a) AND/OR Graph

It is an intuitive method to represent the disassembly process of an EoL product [69]. Fig. 6(a) and (b) show an EoL EV LIB and its AND/OR graph for disassembly [70].

The AND/OR graph is symbolised below.

$$G = (V, E) \tag{1}$$

where $V = \{V_1, V_2, \ldots, V_N\}$ is the set of nodes, and V_i labels a specific subassembly of the EV LIB (e.g., V_{13} in Fig. 6(b) is a subassembly consisting of F (structure frame) and G (battery module)); N is the total number of nodes in V, i.e., the number of the subassemblies of the product; $E = \{e_{j-k}\}$ is the set of edges, and e_{j-k} represents a specific disassembly operation making the subassembly V_j to be V_k (e.g., e_{1-2} in Fig. 6(b) represents a disassembly operation to remove part A from the subassembly ABCDEFGHIJ to form the subassembly BCDEFGHIJ); 'AND' means two operations need to be performed at the same time (e.g., e_{1-2} and e_{1-16} in Fig. 6(b) satisfy an 'AND' relationship); 'OR' indicates that a subassembly has multiple choices of disassembly operations, and each of them can be independently executed (e.g., in Fig. 6(b), V_1 can be disassembled into V_2 and V_{16}, or into V_3 and V_{14}).

AND/OR graphs have been proven to be a valuable tool for modelling and prioritising disassembly operations. Min et al. [71] introduced a weighted AND/OR graph, where the weights assigned to each node represent the cost associated with the corresponding disassembly operation. Chen et al. [72] modelled an EoL product with a transformed AND/OR graph. It uses nodes to represent disassembly operations to provide a clearer understanding of the priority relationships amongst disassembly operations. Tian et al. [55] designed an AND/OR graph to establish priority relationships between disassembly operations in EoL radio products. Bentaha et al. [56] employed an AND/OR graph to represent the disassembly planning of EoL rigid castors. Ren et al. [57] adopted an AND/OR graph to analyse the structure of the HG5–20 three-axis five-speed mechanical transmission product. In this research, to optimise the disassembly processes, an improved genetic algorithm based on the AND/OR graph was designed. For HRC-based disassembly, Xu et al. [58] designed an AND/OR graph to model the disassembly information of a hammer drill. Liu et al. [59] constructed an AND/OR graph for a washing machine, and the Q-learning algorithm was introduced to learn the task allocation strategy between humans and robots during their HRC disassembly. Jin et al. [73] designed a task-based dynamic transformed AND/OR graph to address uncertainties in HRC-based disassembly processes. It can generate suitable disassembly plans under different working conditions by constructing detailed disassembly operations and subtask node graphs. The first available research on disassembling an Audi Q5 hybrid battery system is from [74]. In this study, a disassembly priority matrix and a disassembly priority graph were developed.

However, it is challenging to use AND/OR graphs to represent complex disassembly details. Specifically, it is difficult to clearly express the disassembly priorities of operations located at the same level. Applying AND/OR graphs to model EoL products with numerous parts may lead to the problem of combination explosion. This complexity is evident in some EV LIB representations, as exemplified by the 2017 Chevrolet Bolt battery, which comprises 76 distinct parts and 374 fasteners [18]. Moreover, AND/OR graphs are unable to incorporate more information from economic, environmental, and safety perspectives to support holistic disassembly decision-making processes. In summary, although AND/OR graphs demonstrate some attractive characteristics, more improvements are expected to model intricate EV LIB disassembly processes.

a) Petri Net (PN)

To model the disassembly relationship of a spent product, PN was

Table 5
Summary of related research on disassembly process modelling.

Models	Advantages	Disadvantages	Applications	LIB Disassembly
AND/OR Graph	• Intuitive • Suitable to represent product structures with relatively simple relationships • Ability to record all feasible disassembly sequences	• Too many parts can lead to a combinatorial explosion • Unclear precedence relationship between disassembly operations • Difficult to include more information (time, cost, etc.)	• Tian et al. [55]: radio products • Bentaha et al. [56]: rigid castors • Ren et al. [57]: HG5–20 three-axis five-speed mechanical transmission • Xu et al. [58]: hammer drill • Liu et al. [59]: washing machine	• Difficult for modelling complex LIBs • Combination explosion for complex product modelling
Petri Net	• Intuitive • Suitable to represent product structures with relatively simple relationships • Ability to express more information (operator, time, etc.)	• Too many parts can lead to a combinatorial explosion • The modelling process is more complicated	• Guo et al. [60]: copying machine • Guo et al. [61]: radio set • Ren et al. [62]: hybrid Li-ion battery pack • Tang et al. [63]: obsolete personal computer • Mao et al. [64]: aircraft engine	• Complicated for modelling complex LIBs • Combination explosion for complex products
Matrix-based	• Diversity • Fully express product structure and disassembly processes • Suitable for automated data processing	• Not intuitive • Modelling is more complex	• Parsa et al. [65]: fuel pump • Xu et al. [66]: computer case • Xu et al. [67]: bearing coupler • Wu et al. [68]: Tesla Model S-battery modules	• Suitable for modelling LIB disassembly • Can express comprehensive disassembly information

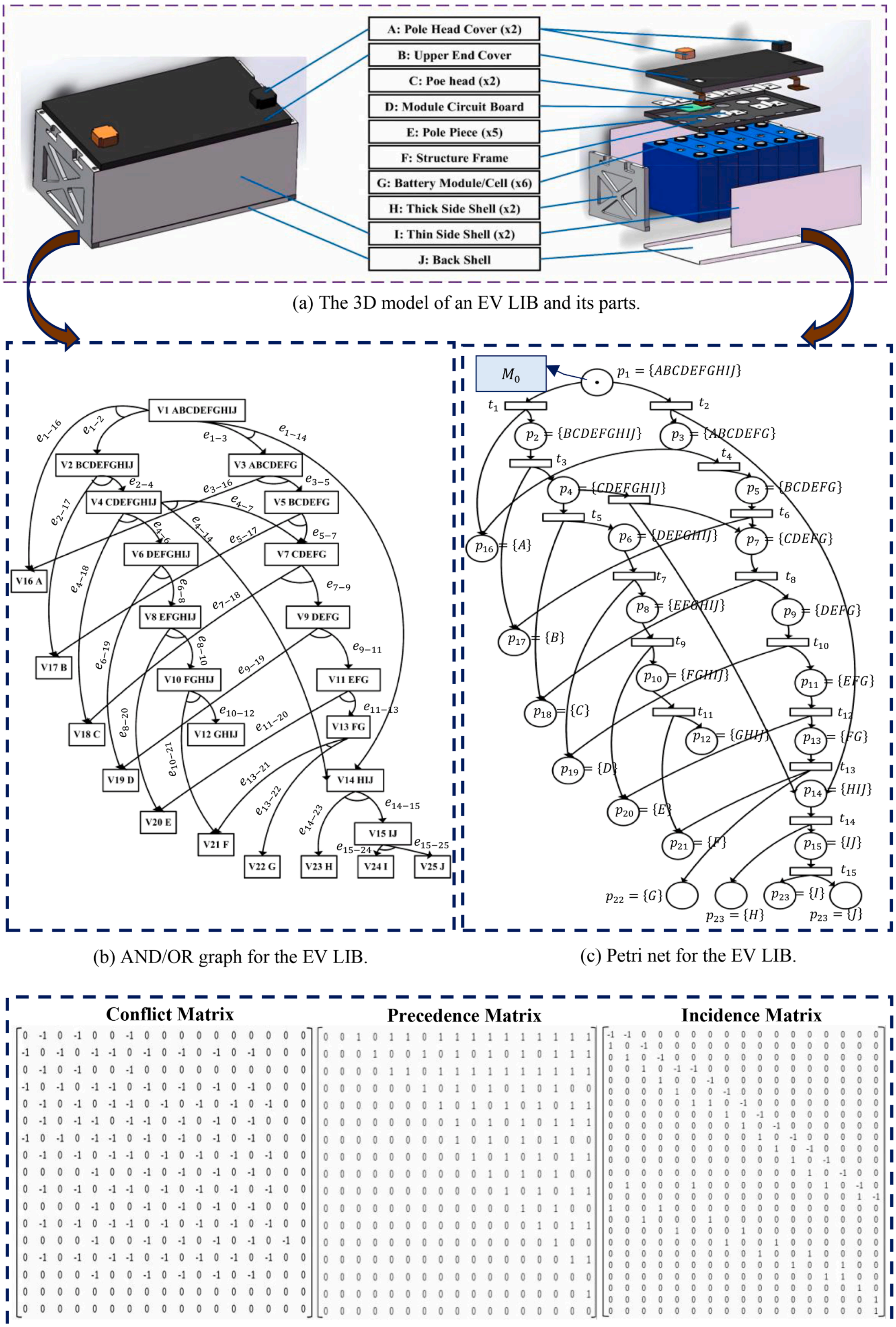

(a) The 3D model of an EV LIB and its parts.

(b) AND/OR graph for the EV LIB.

(c) Petri net for the EV LIB.

(d) Matrices-based modelling for the EV LIB.

Fig. 6. Several disassembly modelling methods for an EV LIB [70].

developed [75]. Fig. 6(c) represents the disassembly PN of the EV LIB shown in Fig. 6(a). It can be defined as the following five tuples:

$$PN = (P, T, I_{n*m}, O_{m*n}, M) \tag{2}$$

- $P = \{p_i | 1 \leq i \leq n\}$ represents the set of places, where each place p_i corresponds to a subassembly/part of a product denoted by the circle in Fig. 6(c), and n is the number of subassemblies/parts;
- $T = \{t_j | 1 \leq j \leq m\}$ denotes the set of transitions, where each transition t_j represents a disassembly operation, and m is the number of disassembly operations;
- $I : P \times T \rightarrow \{0,\ 1\}$ is the input function that defines a set of directed arcs from P to T: 1 indicates the presence of a directed arc, whereas 0 indicates its absence;
- $O : T \times P \rightarrow \{0,\ 1\}$ is the output function that defines a set of directed arcs from T to P: 1 indicates the presence of a directed arc, whereas 0 indicates its absence;
- $M : P \rightarrow \{0,\ 1\}$ represents the token in each place p_i denoted by a dot in the circle in Fig. 6(c), the set M can be used to effectively express the disassembly progress, the initial disassembly status denoted as M_0 indicates that only the place p_1 has been obtained, and the execution of disassembly operations leads to changes in M.

PN can be extended based on specific disassembly objectives and requirements (as shown in Table 6). Guo et al. [60] designed a diversified PN model that integrates the disassembly cost for each transition (disassembly operation) and the recovery value for each place (subassembly). This allows for a comprehensive analysis of the economic aspects of the disassembly process. In another study by Guo et al. [61], the PN model was enhanced by incorporating disassembly resources needed for each operation, such as disassembly tools and operators. The integration facilitates the calculation of costs and time associated with resource changes between different disassembly operations, thereby providing a comprehensive assessment of the overall disassembly process. Ren et al. [62] expanded the capabilities of PN by incorporating the end-of-life status of subassemblies, including reuse, remanufacturing, recycling, and disposal statuses. Corresponding operations were defined in the transitions. To address disassembly uncertainties resulting from human interventions, Tang et al. [63] developed a fuzzy attribution PN model. This model introduced a place set that included human operators and established a fuzzy function that related the operators to disassembly time, cost, and quality. To alleviate the computational complexity, Mao et al. [64] classified the disassembly difficulty, disassembly cost, and disassembly time into multiple levels and integrated them into a PN. Based on this, a reinforcement learning algorithm was developed to optimise the disassembly process.

Table 6
Summary of PN-based disassembly processes.

Ref.	Descriptions	Research contributions
Guo et al. [60]	Incorporated disassembly costs for each transition and part recovery value.	It helped to calculate the costs and benefits of an entire disassembly process.
Guo et al. [61]	Integrated disassembly resources needed for disassembly operations into a PN.	It helped to calculate the costs and time generated due to resource changes between different disassembly operations.
Ren et al. [62]	Defined the end-of-life status of subassemblies in each place, including reuse, remanufacturing, recycling, and disposal, and defined corresponding operations in transitions.	It helped to consider the comprehensive recycling profit of the entire disassembly process of a spent product.
Tang et al. [63]	Developed a fuzzy attribution PN model to mathematically express disassembly uncertainties arising from human interventions.	It considered the influence of different operators on the disassembly process.
Mao et al. [64]	Integrated disassembly difficulty, disassembly cost and disassembly time into a PN by dividing them into multiple levels.	It helped to reduce computational difficulty.
Grochowski et al. [76]	Developed a hybrid Bayesian network grounded in a disassembly PN.	Discerned and deduced interactions amongst defect rates in parts and subassemblies.
Tang et al. [77]	Learned a fuzzy inference system to predict disassembly time and disassembly revenue.	Disassembly knowledge deduced from historical data is more accurate.

The integration of machine learning techniques with PN can introduce innovative strategies for managing the intricate uncertainties in disassembly processes. For instance, Grochowski et al. [76] developed a hybrid Bayesian network grounded in disassembly PN to deduce defect rates in parts and subassemblies, thereby contributing to the formulation of informed disassembly plans. Ren et al. [62] explored issues related to the reprocessing of parts of spent products through maximum likelihood estimation. Tang et al. [77] introduced an adaptive learning system for predicting disassembly operation time and part revenue using a fuzzy disassembly PN. It utilises input parameters such as part quality status and operator skill level.

PN is generally considered more flexible than the AND/OR graph for several reasons. First, PN can strictly respond to a disassembly process by using tokens. These tokens represent the progress and state of disassembly operations, providing a clear visual representation. Moreover, PN enables the specification of human operators who are responsible for disassembly operations, and various disassembly criteria, such as disassembly time, cost, and quality, can be included in the transitions. This level of detail enhances the expressiveness and analytical capabilities of PN for disassembly processes. Furthermore, PN can express the uncertainties in disassembly processes by incorporating methods such as machine learning. It is of utmost importance to spend time on LIB disassembly processes, as there are many uncertainties. However, constructing a PN model is much more complex than constructing an AND/OR graph. This complexity becomes more apparent when processing LIBs with a large number of parts, which can lead to combinatorial explosion problems.

a) Matrix-based Modelling

Matrix-based modelling constitutes an exceptionally efficacious technique for elucidating the disassembly progression of intricate products that comprise a multitude of parts. Within the framework of Fig. 6(d), several matrices are depicted, serving as a representation of the disassembly process for an EoL EV LIB. amongst these matrices, a significant one is the disassembly precedence matrix. It is a matrix routinely employed to delineate the sequential relationship between disassembly operations [65]. In actual disassembly, the precedence matrix may be more complicated due to the non-negligible disassembly directions. Depending on the spatial location relationship of the parts in the CAD model of the spent product, the disassembly precedence of the components in the six directions (x+, x-, y+, y-, z+, z-) may be different [78]. To cope with changing conditions, a dynamic disassembly priority matrix was designed [79]. The conflict matrix describes the conflict relationship between the disassembly operations [71].

Matrix-based modelling can also represent the uncertainty of part quality during disassembly. For instance, Laili et al. [80] analysed three types of part deformation (enlargement, contraction, and bonding), and a probability matrix was established to express the probability of occurrence of each type for each part. Based on this, an interference probability matrix was obtained, where each element expressed the probability of interference between two parts of the spent product. Similarly, Ye et al. [81] analysed the uncertain interference relationship between parts in the disassembly process and established a feasibility matrix and a confidence matrix. In the field of HRC-based disassembly modelling, matrix-based methods have gained popularity and have been applied in various studies. Xu et al. [66] employed matrix-based modelling to represent a retired computer case. Matrices were established to express the structural relationships between fasters and parts, including stability relationships, contact relationships, and interference relationships. By leveraging these matrices, a feasible task sequence for HRC-based disassembly was generated to optimise the disassembly process. In another study, Xu et al. [67] developed two matrices to capture the AND/OR relationship between disassembly operations in an EoL bearing coupler. This matrix-based representation facilitated the depiction of the interdependencies amongst disassembly operations, enabling efficient planning and sequencing of operations. Similarly, Wu et al. [68] used a disassembly operation priority matrix to depict the disassembly process of Tesla Model S battery modules.

In summary, the matrix-based modelling approach has the following advantages: (1) by increasing the number of rows and columns of the matrix, the modelling of complex EoL products can be achieved; (2) for uncertainties in disassembly processes, the corresponding probability matrix can be established; and (3) it is more conducive to automated processing (e.g., Zhao et al. [82] constructed a deep network with the matrix model as input and the disassembly decision as output). Therefore, for EV LIBs with complicated structures, matrix-based modelling could be the most suitable for disassembly process representation. It is also convenient to combine with state-of-the-art AI models to facilitate smart reasoning in disassembly processes.

3.3. Refinement for EoL LIB modelling

The disassembly modelling approaches discussed above assume that the complete structures of EoL LIBs have been established. LIBs and composite battery packs are geometrically complex objects, with many features potentially hidden from a one-time sensory survey. It is usually challenging to obtain an accurate and complete model of an EoL LIB. Therefore, it is essential to refine the EoL LIB modelling at runtime and in a rolling-horizon manner. For instance, Adesso et al. [52] used 3D vision to detect parts of an EoL product in real time during disassembly, prioritising the removal operations for fasteners based on detection results. ElSayed et al. [83] implemented an online detection approach for an EoL computer using a 2D image template matching algorithm. A new disassembly route is replanned when there are newly detected parts. A hybrid graph model was designed to describe the contact, priority, and hierarchical relationships in an EoL product for disassembly [82]. The graph is continuously updated when there are missing or additional parts identified in the product. Laili et al. [84] designed a two-pointer detection strategy to establish a disassembly interference matrix to quickly identify removable parts when a disassembly operation fails. Notably, the above approaches developed for other EoL products can be effectively applied to model LIBs for disassembly in an incremental refinement way. It will address the challenges arising from the variability and condition of EoL LIBs.

4. HRC-based disassembly planning for LIBs

The disassembly of LIBs usually takes place in a complex, uncertain, and hazardous environment, rendering complete manual or robotic disassembly impractical. Furthermore, bespoke disassembly systems may fail in such complicated scenarios because of a lack of flexibility to deal with uncertainty. However, the HRC-based disassembly system leverages the synergistic strengths of humans and robots, combining human dexterity, high perception, and intelligence with the strength, endurance, and precision of robots. As a result, effective planning for HRC-based disassembly systems for LIBs becomes paramount. Addressing the problem of HRC-based disassembly planning comprehensively involves two aspects: (1) Allocating disassembly tasks to either humans or robots. This entails elucidating the characteristics of the disassembly tasks and discerning their suitability for either human or robotic execution; (2) Planning HRC-based disassembly processes. This planning procedure entails the judicious sequencing of disassembly tasks for humans and robots, aligning with the overarching objectives of the disassembly process. Each of these issues will be discussed in the subsequent subsections.

4.1. Disassembly task allocations for HRC

A LIB pack consists of multiple modules, and each module contains numerous cells. These elements are connected together according to some typical configurations and hierarchical structures using mechanical, electrical, thermal, and/or chemical joining techniques [11]. Each disassembly task of a LIB entails multiple options of operations, each exhibiting different levels of difficulty, complexity, cost, risk, etc. They are useful indicators or criteria to facilitate the decision-making process about whether the disassembly task should be performed by a human or delegated to a robot. For instance, intricate disassembly tasks are more suitable for human intervention, whereas hazardous and repetitive tasks are more appropriately handled by robots. In this subsection, the current research on disassembly task assignments for humans and robots is discussed. A summary is shown in Table 7.

Wegener et al. [27] designed a novel HRC-based disassembly framework designed for the systematic disassembly of an Audi Q5 hybrid battery. The disassembly processes span from the battery pack to the battery cell. The framework meticulously delineates each disassembly operation, providing detailed insights into the involved tasks, disassembly tools, and designated operators responsible for their execution. Cheng et al. [85] developed an approach for evaluating HRC-based disassembly capabilities. The model incorporates indicators from the perspective of economic, social, and environmental benefits. First, data were collected from real-world disassembly workshops according to these indicators. Then, the principal component analysis (PCA) algorithm was used to combine historical and real-time data. Furthermore, the analytic hierarchy process (AHP) algorithm was developed to assign weights to the indicators. Finally, the disassembly capabilities of various humans and robots were ranked. Li et al. [86] classified disassembly tasks into three categories, namely, H-type (requiring human intervention), R-type (requiring robotic intervention), and H/R-type (allowing for either human or robotic intervention). Disassembly tasks were determined by six indicators, namely, high complexity, uncertainty, toxicity, repetitiveness, heavy load capacity, and other factors.

While the above methods provide a qualitative framework for classifying disassembly tasks, it lacks quantitative analysis. To address this issue, Hellmuth et al. [18] introduced a method for the automated assessment of EV LIB disassembly. The method comprises two evaluation categories, where the first pertains to the feasibility of automating disassembly operations, and the second focuses on determining the necessity of automation. Within each category, five criteria are considered. Based on the scores assigned to each criterion, it is determined whether a disassembly operation should be executed by a robot or a human. Parsa et al. [65] defined eight parameters for disassembly tasks, each of which was assigned a degree value by experts. These parameters include part size, part weight, part shape, disassembly tool requirements, accessibility, disassembly operational complexity, disassembly positioning, and disassembly operational force. By further adding up all the parameter values, tasks with scores higher than the mean are highly complex tasks that are assigned to humans to carry out. Furthermore, Xu et al. [67] and Liu et al. [87] identified four categories of disassembly tasks. In addition to the H-type, R-type, and H/O-type, there is also the $O + R$-type. This new type involves disassembly tasks jointly completed by a human and a robot. To classify these disassembly tasks, a classification regression algorithm was developed by considering some parameters, such as part weight, part volume, precision needed for disassembly, and types of disassembly tools used.

Table 7
Summary of research on disassembly task assignment for HRC.

Ref.	Indicators for task assignment	Characteristics	Applications
Wegener et al. [27]	Complexity	Simple, qualitative analysis	Audi Q5 hybrid batteries
Cheng et al. [85]	Economic; social; and environmental benefits		Computers
Li et al. [86]	High complexity; uncertainty; toxicity; repetitiveness; heavy load capacity; and other factors		Gear pumps
Hellmuth et al. [18]	Feasibility of automating the disassembly operations; necessity of automation	Comprehensive consideration and quantitative analysis	EV LIBs
Parsa et al. [65]	Component size; component weight; tool requirements; accessibility; component shape; operational complexity; positioning; and operational force		Fuel pumps
Xu et al. [67] and Liu et al. [87]	Part weight; part volume; precision needed for disassembly; and types of disassembly tools used		Bearing couplers
Xu et al. [58]	A variable called K to represent the difficulty level of a disassembly operation	Simple, lack of analysis of K	Hammer drills
Xu et al. [66]	For robots: perception ability, operation area, and movement complexity For humans: workload and hazard level	More reasonable due to distinguishing between humans and robots	Computer cases
Guo et al. [88]	Part attributes (such as size and weight); disassembly process (including tool requirements and operational complexity); and HRC environment (including risks of spatial collisions and chemical hazards)	Comprehensive consideration and quantitative analysis	Automobile engines
Liu et al. [89]	Disassembly depth complexity; disassembly process complexity; and disassembly decision complexity	More practical due to learning network models	Automotive traction batteries of Model 1

In addition, some studies have attempted to categorise disassembly tasks based on their levels of difficulty. Xu et al. [58] used a variable called K to represent the difficulty level of a disassembly operation. If $K > 10$, then the operation is assigned to a human, whereas if $K < 10$, the operation is assigned to a robot. However, the study did not provide a clear explanation for how the K value is determined. In contrast, Xu et al. [66] defined two separate sets of criteria for evaluating the difficulty of disassembly tasks for a human and a robot. For a robot, the difficulty level is defined based on three attributes, namely, perception ability, operation area, and movement complexity. For a human, the difficulty level is determined by two attributes, namely, workload and hazard level. Each attribute is assigned a value between 0 (none) and 1 (extreme). The overall disassembly difficulty is calculated by taking the maximum value of the respective attributes. Guo et al. [88] defined the disassembly difficulty by considering three factors, namely, part attributes (e.g., size and weight), disassembly process (e.g., disassembly tool requirements and operational complexity), and HRC environment (e.g., risks of spatial collisions and chemical hazards). The disassembly difficulty value is calculated by taking the maximum score for each of the above factors assigned by experts. Liu et al. [89] investigated the complexity of disassembly tasks and established three disassembly complexity metrics, namely, disassembly depth complexity, disassembly process complexity, and disassembly decision complexity. To classify disassembly tasks, a multilayer perceptron neural network was built using complexity indicators as input and task categories as output.

Most of the assignment methodologies of disassembly tasks between humans and robots are typically based on the attributes of the disassembly task itself. Recently, ergonomic considerations have gained prominence [90]. Human factors, such as human safety, work comfort, and psychological well-being, should be considered to ensure that disassembly processes are not only efficient but also safe and comfortable for humans. Chen et al. [91] used the bending angle of the human body as a metric to assess human comfort during disassembly processes. By taking these considerations into account, advanced HRC-based LIB disassembly systems with human factor considerations can be developed.

4.2. HRC-based disassembly planning

In HRC-based disassembly, two prominent planning problems are the disassembly operation sequencing planning (DOSP) problem and the disassembly line balancing (DLB) problem. The DOSP problem focuses on determining the optimal sequence of disassembly operations at a given workstation, whereas the DLB problem involves the allocation of disassembly operations across multiple workstations in a disassembly production line [92,93]. A summary of HRC-based disassembly planning research is shown in Table 8.

To address the planning problem, it is necessary to define HRC-based disassembly planning objectives. For the HRC-based DOSP problem, objectives include minimised disassembly time, disassembly cost, disassembly difficulty, and maximising disassembly safety. The disassembly time can be divided into two main parts, namely, basic disassembly time and additional disassembly time [66,88]. The former represents the cumulative duration needed for disassembling each part by the human and the robot, whereas the latter comprises various contributing factors, including disassembly tool changes, directional adjustments, the movement of the robot and human across different disassembly positions, and any waiting time for other high-prioritised disassembly operations [7,8,10]. Significantly, during practical disassembly operations, the specific duration of a human's disassembly time often remains uncertain [94]. Previous research considered this uncertainty factor by employing either normal distributions [95] or triangular fuzzy functions [94]. In addition, Li et al. [86] introduced a model that establishes the relationship between a human's disassembly time and the level of fatigue experienced, thereby suggesting a positive correlation between increasing fatigue and prolonged disassembly time. Disassembly costs encompass a comprehensive calculation that involves the multiplication of the hourly labour cost with a human's disassembly time, in addition to the hourly maintenance cost of a robot with its operating time [66,96]. Moreover, the level of difficulty is related to the process of executing diverse disassembly operations by both a human and a robot. As a result, numerous studies have been dedicated to establishing specific criteria to assess the difficulty of disassembly tasks for both humans and robots [66]. Ensuring disassembly safety is another critical consideration in the HRC-based DOSP problem. Liao et al. [97] used strain index (SI) score as an indicator of human safety. It can assess the risk of musculoskeletal disorders in the distal upper limbs of a human, including the hand, wrist, forearm, and elbow. When planning the sequence of disassembling screws on spent products by a human and a robot, Zhou et al. [21] defined human safety as one of the planning

Table 8
Summary of HRC-based disassembly planning research.

Ref. and Problem	Planning Objectives	Optimisation	Cons and Pros
Xu et al. [66], DOSP	• Disassembly time • Disassembly cost • Disassembly difficulty	Modified discrete Bees algorithm based on Pareto	• Wide application • Fast learning speed • Inability to adapt to dynamic disassembly environments
Guo et al. [88], DOSP	• Disassembly time • Disassembly cost	Genetic algorithm	
Li et al. [86], DOSP	• Disassembly time	Bees algorithm	
Parsa et al. [65], DOSP	• Disassembly time • Nontargeted component index	Genetic algorithm	
Xu et al. [67], DLB	• Number of disassembly workstations • Smoothness index of disassembly time • Demand index	Improved discrete Bees algorithm	
Liu et al. [87], DLB	• Number of workstations • Smoothness index • Disassemble high-demand parts as early as possible	Improved discrete Bees algorithm	
Wu et al. [68], DLB	• Number of needed workstations • Smoothness of the load between workstations • Number of manual workstations • Cost of disassembly	NSGA-II	
Xu et al. [58], DLB	• Disassembly profit • Disassembly consumption • Disassembly difficulties • Number of workstations	Artificial bee colony algorithm	
Xiang et al. [98], DLB	• Disassembly profit	Multi-neighbourhood parallel greedy search algorithm	
Zhou et al. [21], DOSP	• Disassembly time • Disassembly safety	Stackelberg model	• Adaptation to dynamic disassembly environments • Limited application • Complex modelling
Liu et al. [59], DOSP	• Disassembly time	Q-learning algorithm	

objectives. The safety level was evaluated by the minimum distance between the human and the robot during disassembly processes. The smaller the distance is, the higher the safety level.

The DLB problem refers to the allocation of disassembly operations to multiple HRC-enabled disassembly cells to achieve predefined disassembly objectives. An HRC disassembly cell consists of a human operator and a robot. Minimised disassembly time, disassembly cost, and disassembly difficulty are common objectives in DLB problems. Specifically, reducing the number of needed workstations is often an objective to lower overall costs. Increasing the evenness of the workload on each workstation is also an effective means to reduce idle time and costs. Furthermore, the number of manual workstations should be optimised to minimise human fatigue levels and reduce the risk of injury [68]. Disassembly time is generally defined as cycle time to represent the maximum time spent by a disassembly workstation to dismantle a product [73]. In addition, disassembly profits are generally obtained by subtracting the costs incurred by humans and robots from the total value of disassembled parts [98].

When planning objectives have been determined, an appropriate optimisation algorithm should be established to solve both the HRC-based DOSP and DLB problems according to the objectives. Both problems are NP-hard, which means that no economically and technically reliable solution can be identified even when an exhaustive search approach is used. Therefore, most of the research works have used metaheuristic algorithms to optimise the two problems. Metaheuristic algorithms, which imitate the behaviour of creatures in nature, have been commonly employed to solve combinatorial optimisation problems. In HRC-enabled disassembly planning, the bees algorithm (BA) is frequently employed [66,67,86,87]. This algorithm utilises scout bees to explore new solutions to pursue global optimisation, while follower bees focus on exploring nearby solutions for local optimisation. Another popular approach is genetic algorithms, as evidenced by their use in several studies [65,68,88]. To tackle multiobjective problems in HRC-based disassembly planning, there are two main approaches. The first is to convert a multiobjective problem into a single-objective problem by weighting different objectives. However, this approach is greatly affected by weights, so there is no guarantee that each objective can be optimised. The second is to employ the Pareto algorithm to combine different metaheuristic algorithms. It provides a good balance between various disassembly objectives. Some examples of such algorithms are BA based on Pareto [66] and NSGA-II [68]. Additionally, algorithms such as the artificial bee colony (ABC) algorithm [58] and the greedy algorithm [94] were also utilised in certain studies, albeit less frequently.

However, plans derived by metaheuristic algorithms are fixed and not adaptive to dynamic HRC-based LIB disassembly environments, e.g., uncertain product quality [99], uncertain product structure [77], uncertain human intervention, etc. Therefore, several studies have suggested the use of agent-based approaches to resolve dynamic disassembly planning problems. Agent-based approaches differ from metaheuristic algorithms in that they implement disassembly planning decisions step-by-step by sensing the environment rather than providing a complete disassembly plan at the beginning. Zhou et al. [21] modelled a human and a robot as separate agents in disassembly processes, and a Stackelberg game model was designed to plan their disassembly actions in real time. The Stackelberg model is a human-centric game model that ensures the profit of humans during disassembly processes. Liu et al. [59], on the other hand, applied a reinforcement learning (RL) algorithm based on Q-learning to solve disassembly decisions for both humans and robots. In the approach, a disassembly task is used as the disassembly state, the execution of the disassembly task is used as an action, and the negative value of the disassembly time is used as a reward. This enables the total disassembly time to be optimised. In general, agent-based approaches have high requirements for model formulation skills and are therefore only applicable to highly complicated and dynamic problems.

In addition, there are some approaches to disassembly replanning in the field of non-HRC-based disassembly planning. For instance, Laili et al. [84] introduced a ternary bee algorithm designed to identify novel disassembly sequences and directions. This algorithm efficiently combines the advantages of greedy search and heuristic algorithms, enabling rapid exploration of new planning solutions. Zhao et al. [82] employed deep Q-networks to generate dynamic disassembly solutions. Vongbunyong et al. [100] developed a robotic disassembly system with learning and revision capabilities. This system accumulates product-specific disassembly knowledge and invokes appropriate disassembly strategies from the knowledge base for different structures of disassembled products. This facet represents a promising avenue for future research, offering the prospect of applying these methodologies to the realm of HRC-based disassembly planning and replanning.

In the future, comfort, mental health, and psychological stress experienced by humans during the disassembly process should also be considered as optimisation objectives. State-of-the-art deep learning and RL technologies can be explored and applied when planning the disassembly process to provide a fast, model-free, intelligent disassembly decision.

5. HRC-based disassembly operations

LIBs consist of multiple parts that are joined by various means. The disassembly processes of a LIB require disconnecting individual parts. There are two types of joins in LIBs. The first is permanent joining, such as bonding and welding. Part separation can only be undertaken through destructive disassembly technologies, such as cutting, pulling, impact, or hot melting. The second is non-permanent joining, such as screw connections, pinhole connections, and snap-fit connections. They can be dismantled using non-destructive technologies.

The disassembly process of a LIB involves disconnection operations of the pack, modules, and cells in the LIB. To conduct the operations, destructive disassembly has been a prevailing practice. The disassembly phase of the battery pack includes cutting cable ties, cutting cooling pipes, and cutting bonded battery modules and the battery bottom cover for separation [101]. Similarly, during the disassembly phase of battery modules, cutting operations are used to separate battery cells bonded together with adhesives and electrical connectors between battery cells connected through welding methods [102]. In the process of disassembling battery cells, various components, including cathodes, anodes, compounds, separators, etc., also necessitate the utilisation of cutting operations for separation. Presently, despite the escalating demand for automation in destructive disassembly processes, a considerable portion of these procedures is still performed manually. AI and robotics are catalysing a transformative shift towards automated destructive disassembly. Schäfer et al. [103] developed a mechanical milling device designed for the removal of electrical connectors between battery cells. Through experimental validation, they demonstrated that a milling depth of 0.3 mm proved effective in disconnecting the electrical connectors without causing damage to the battery. Li et al. [104] developed a mechanical apparatus for the automatic dismantling of pouched LIB cells. It can successfully disassemble cathode sheets, anode sheets, separators, and polymer-laminated aluminium film housings. Kay et al. [29] employed a robot to operate a high-speed rotating cut-off wheel to cut the battery module housing in order to obtain a complete battery cell. Lu et al. [105] used real-time temperature data collected by a thermal imager to establish a long-short-term-memory (LSTM) model to predict the cutting temperature pattern when using a cutting tool on battery cells. Subsequently, cutting parameters are adjusted through closed-loop control to prevent damage to the battery cell caused by excessive temperature.

Nevertheless, the current trajectory in the field of disassembly emphasises the sustained pursuit of automated non-destructive disassembly techniques [106]. This emphasis stems from the recognition that the utilisation of destructive disassembly methods incurs elevated customisation costs and jeopardises the integrity of components, diminishing their potential for subsequent reuse and refurbishment. Furthermore, considering the challenges associated with non-destructive disassembly for LIBs, which include unstable factors, such as rusty parts, hazardous liquid leakage, and part shape changes, a smarter and more flexible disassembly operation is imminent. In the following, major non-destructive disassembly mechanisms and technologies for LIBs will be analysed.

5.1. Disassembly mechanisms of different non-destructive connections

Some commonly used non-destructive connection structures in LIBs include screw connections, peg-hole connections, and snap-fit connections. Disassembly mechanism analyses for the connections are illustrated in Fig. 7.

Lander et al. [95] analysed the disassembly process of six commercial packs from Renault, Nissan, Tesla, BAIC, Peugeot, and BYD. It was concluded that unscrewing is one of the predominant disassembly operations during LIB disassembly. Using the BAIC battery pack as an example, 29% of the total disassembly time was spent on screw removal. After acquiring the positional data of a screw through visual inspection or the CAD model, it becomes necessary to further refine the disassembly process. In this regard, force plays a crucial role, as it serves as both an essential input for robotic position control and a significant output for robotic force control. For instance, when dealing with a hexagonal screw in a spent product, Li et al. [110] designed an automated screw-loosening process using a robot. This process involved real-time detection of the contact force between the screwdriver on the robot and the screw, allowing the screwdriver to compliantly approach the screw. Subsequently, a spiral search strategy was devised to ensure proper engagement of the screwdriver head with the screw. To gain a clearer understanding of the needed control force for screw disassembly, Mironov et al. [107] conducted experiments to investigate haptic patterns employed by human operators during unscrewing tasks (as shown in Fig. 7(a)). The research revealed that humans exert an axial force on screws to prevent screwdriver slippage. Moreover, it was observed that the magnitude of the axial force applied is directly proportional to the needed unscrewing torque. Huang et al. [111] identified three common failure modes encountered when dealing with damaged or rusted screws, namely, missing the screw with the screwdriver, the screwdriver slipping on the screw surface, and encountering screws that are too tightly fastened to be removed. To address these challenges, they devised solutions to implement spiral searches and loosen movements repeatedly. Additionally, in situations where a robot is unable to complete the unscrewing task, a human operator is notified for assistance. Zhou et al. [10] designed a robotic system to significantly minimise the disassembly time for EoL LIBs. In particular, robotic unscrewing operations supported by the system achieved a time savings of 55%.

Disassembling the peg-hole is closely related to the fit between the peg and the hole. For interference fits, Wang et al. [112] developed a non-destructive disassembly approach that employs cooling excitation using liquid nitrogen. Cooling causes parts to cool and deform, which weakens the interference fit and facilitates disassembly. In the context of clearance fits, Zhang et al. [108] proposed a compliant disassembly scheme and analysed four contact states that occur when extracting a cylindrical peg from a clearance fit hole. These states were no contact, one-point contact, two-point contact, and line contact (as shown in Fig. 7(b)). It is worth noting that the two-point contact state causes the disassembly process to require an extremely large force. To reduce the two-point contact region, through theoretical analysis, it was found that the region was reduced significantly when the compliance centre was at the tip of the peg, which was proven through experiments. Su et al. [113] presented a novel approach to disassembling a peg from a hole through the design of a compliant robotic end-of-arm tool. Unlike the remote compliance centre mechanism used in peg-hole assembly [114], this device is capable of withstanding tension rather than pressure during disassembly, thus enabling the successful removal of the peg without jamming or wedging. Finite element modelling simulations were conducted to validate the efficacy of the tool design.

Snap-fit fasteners, known for their convenience and the requirement of applying only a specific amount of pressure during assembly, have gained popularity for assembling small parts, such as covers of bus bars in LIBs. However, the challenge lies in their disassembly process, which is often complicated due to the varying forces involved. To address this issue, Guo et al. [109] deduced a comprehensive disassembly mechanics

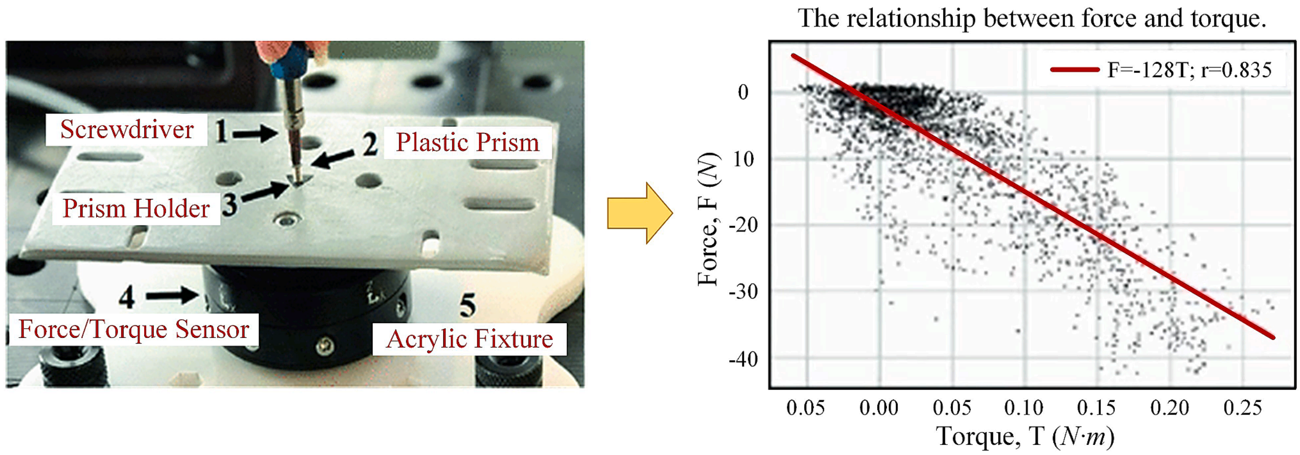

(a) Mechanics analysis of unscrewing processes [107].

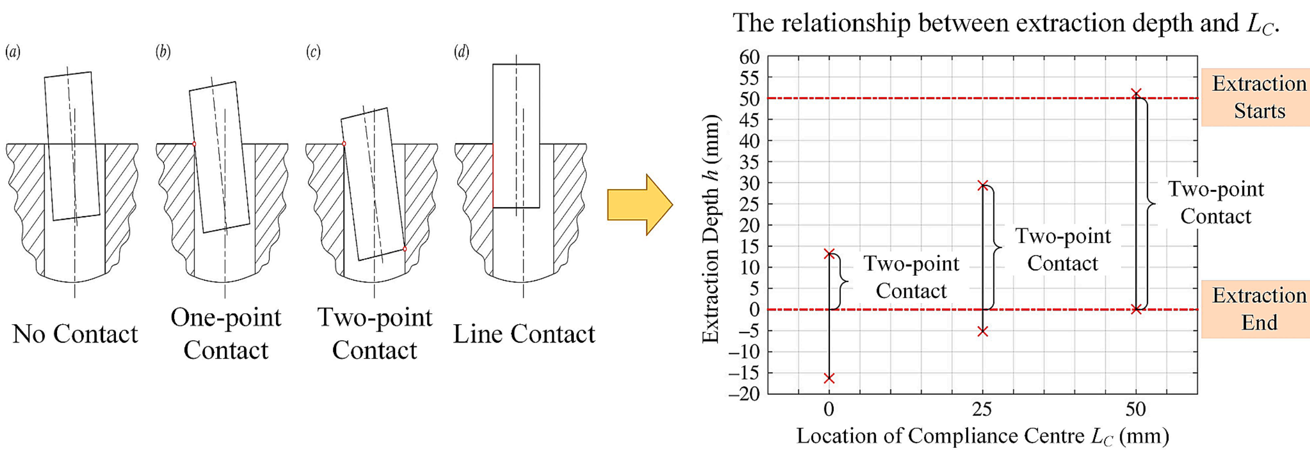

(b) Contact state analysis of removing a peg form a hole [108].

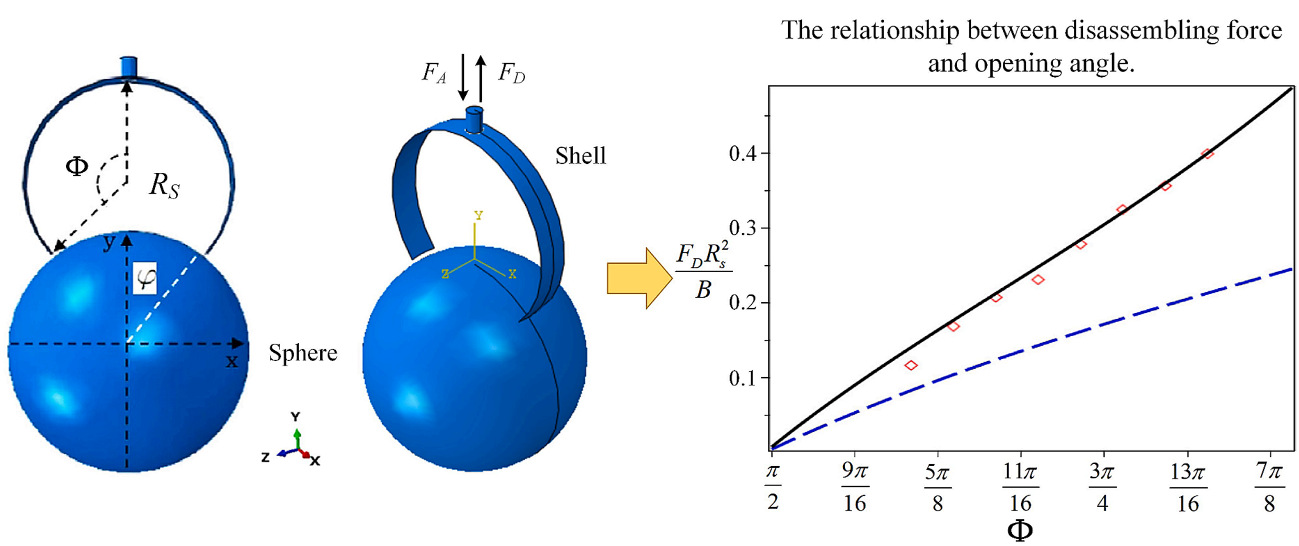

(c) Mechanics analysis of disassembling spherical snap-fit parts[109].

Fig. 7. Analysis of the disassembly mechanisms of different connections.

formula for spherical snap-fit parts. Their analysis revealed the influential role of the key parameters of snap-fit parts, such as the initial opening angle, friction coefficient and radius, on the disassembly force. Notably, an increase in the opening angle directly corresponds to a larger disassembly force (as shown in Fig. 7(c)). To substantiate their theories, the researchers employed finite element analysis and conducted actual experiments, thereby providing evidence for their conclusions. In addition, Schumacher et al. [115,116] developed a disassembly tool specifically designed for cantilever snap-fit fasteners. This tool incorporates a force-sensing tool tip equipped with three force-sensing resistors, enabling horizontal and normal force feedback. The tool effectively pushes and lifts the snap-fit cover along with the spring-loaded batteries it holds, facilitating the disassembly process. Moreover, Carrell et al. [117] explored a novel approach to disassembling snap-fit fasteners from a design perspective. Their approach involved utilising shape memory polymers as the primary constituent material for snap-fit fasteners. When exposed to a thermal field, these shape memory polymers undergo automatic disassembly, eliminating the need for any manual or machine operation. This innovative design feature simplifies the disassembly process and enhances the overall user experience.

In summary, the disassembly technology of various connections has gradually matured. In addition, for uncertain situations that may occur in standard parts, such as rust and inaccurate positions, related research needs to be further improved.

5.2. *Acquisition of robotic flexible disassembly ability for disassembly operations*

Due to the sophistication of the HRC-based LIB disassembly environment, it is critical for robots to possess some flexible disassembly capabilities. While certain standard connection structures can be disassembled using customised tools or specific programming tasks, non-standard parts (such as cables and shells), as well as parts that deform due to environmental influences, pose additional challenges. Successfully disassembling them requires robots to have high flexibility and adaptability. For instance, to remove cables from LIBs, a robot must locate the cable accurately. Subsequently, it needs to analyse the optimal grasping posture and determine the appropriate magnitude of the applied grasping force. After grasping, the robot must ensure that the cable can be securely placed in the correct position [118]. However, each of these operations presents its own challenges. Additionally, the soft and uncertain shape of cables further complicates the disassembly process. Learning plays a pivotal role in enabling robots to possess flexible disassembly capabilities. While the kinematics and dynamics of robots have been extensively studied in theory, practical implementation of robotic manipulation faces challenges due to the nonlinear and unstructured kinematic and mechanical relationships influenced by unknown environments [119]. Machine learning offers a promising approach to addressing these uncertainties and nonlinear relations, providing robots with intelligent perception, adaptive motion control, and knowledge adaptation capabilities [120]. The learning process of robots can be categorised into two types (as shown in Fig. 8), namely, RL, wherein robots acquire knowledge by exploring their surrounding environments, and imitation learning (IL), wherein robots learn by emulating human actions and behaviours.

Robot learning through exploration can usually be expressed as a single Markov decision process (MDP) [121]. Key components in the MDP process include the robot's perception of the environment, its actions, state transition functions, reward functions derived from task objectives, and strategies for determining actions. RL is a widely used approach for acquiring optimal strategies, wherein robots actively interact with the environment and accumulate experiences to maximise returns. The outcomes of this learning process enable robots to execute highly effective operations through astute environmental observations. For instance, Qu et al. [122] designed the deep reinforcement learning (DRL) algorithm to train the robot to remove the door chain bolt from the lock. In the research, the perceived mechanics information is taken

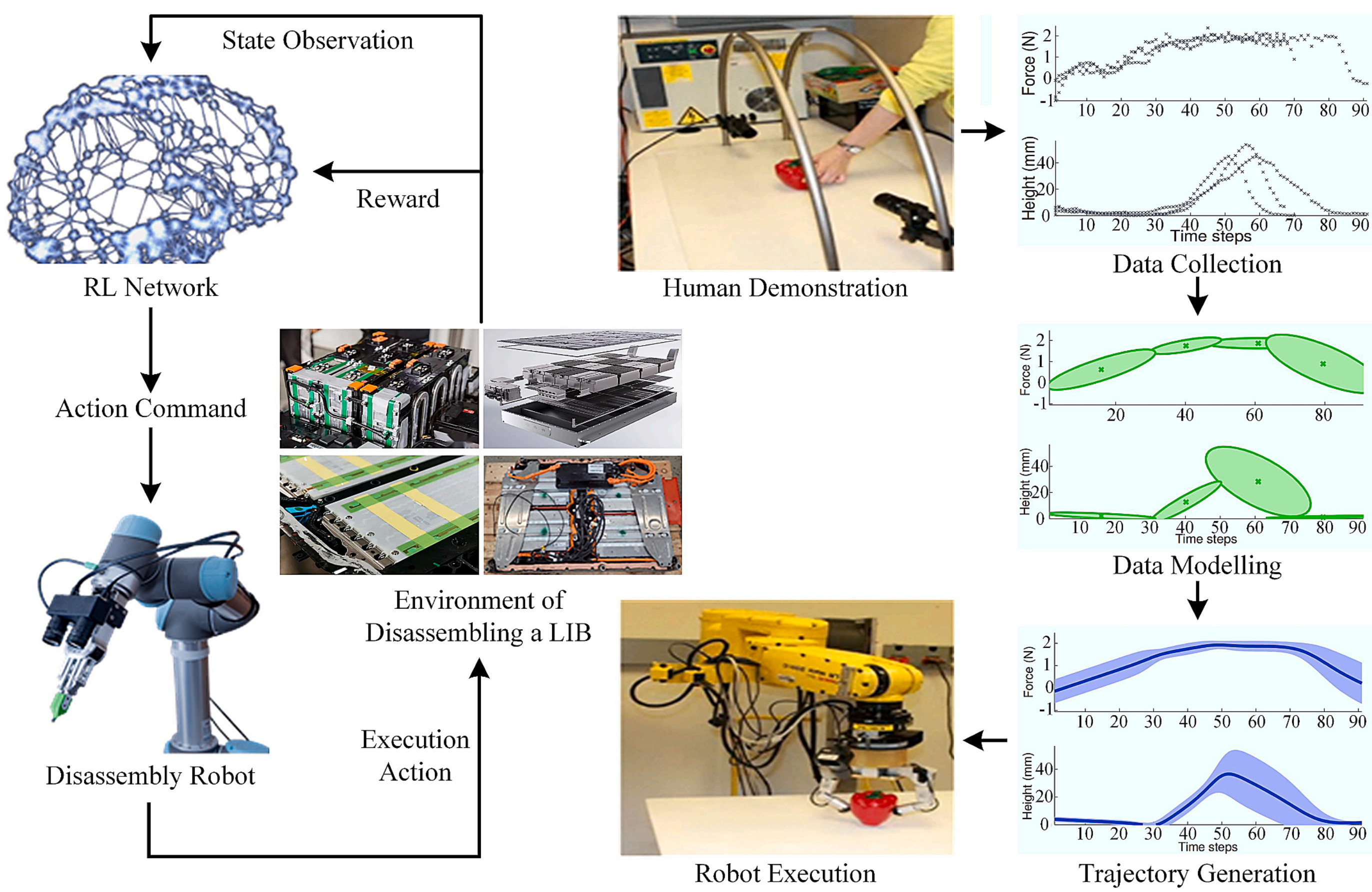

(a) The basic model of RL (b) An example by using IL [138]

Fig. 8. Two types of learning processes for robots to pick up new skills.

as the state input, and the displacement change of the robot actuator is taken as the output. Kristensen et al. [123] developed an RL algorithm for the task of unscrewing. However, MDP modelling demands a comprehensive understanding of the environment, i.e., the ability to obtain exact state information. Yet, in actual disassembly environments, there are limitations to obtaining complete status information. For instance, for a grabbing process, visual information achieved using a camera may be obstructed by obstacles. Therefore, some studies employed partially observable MDP (POMDP) to model such scenarios [124]. POMDP modelling differs in that the state is estimated through observations and expressed in the form of a probability distribution.

Grasping is a prevalent operation in the field of disassembly [125]. In recent years, there has been a growing interest in employing RL to address the challenge of grasping objects with nonstandard shapes. This has significant implications for disassembling LIBs. Presently, the application of RL in grasping methods has shown remarkable progress, enabling robots to achieve 6-degree-of-freedom (6-DOF) grasping [126]. This means that the robot gripper can successfully grasp target objects from specific positions and orientations, thereby enhancing the overall success rate of grasping. For instance, Gualtieri et al. [127] developed an effective MDP model for object grasping in randomly placed environments. The model utilised the point cloud data of objects and positional data of the robot as the state and the adjustment of the angle of the robotic axis joint as the action. Experimental results showed a remarkable 86% success rate in real-world scenarios, particularly for complex objects such as mugs. Hou et al. [128] developed the inclusion of a grasping quality evaluation mechanism and incorporated it into the reward function. This evaluation mechanism is determined by analysing changes in depth images before and after a grasping action. Insignificant changes observed in the images indicate a high-quality grasp. Line-of-sight blocking is a common challenge faced by vision sensors. To address this issue, tactile sensors have been incorporated into grasping scenarios. Wu et al. [129] implemented a gripper with multiple haptic sensors at the robot's end. Within the MDP model, the state representation consisted of the robot's position during motion, the acquired haptic information, and the bending angle of the gripper. In a simulated environment, the experiment achieved a remarkable minimum success rate of 95%. Furthermore, POMDP models have been frequently employed to represent grasping environments while accounting for uncertainties, such as errors in sensing data and unknown properties of the grasped object (e.g., colour, the centres of gravity and position). Hsiao et al. [130] incorporated eight haptic sensors into a robotic gripper to gather information about the object to be grasped and the gripper's position. The grasping space is divided into discrete regions, and haptic information is used to estimate the probability of the gripper and the object being in each region. In a multi-object grasping environment, environmental uncertainty increases exponentially with the number of objects. It introduces challenges like occlusion between objects, making it difficult to determine the position and grasp success. To address this, Pajarinen et al. [131] used an RGB-D camera to observe each object on a table. Independent state variables (colour, position, and grasp success) are created for each object. Observations include information about the position of an object after moving and lifting it. The state probability distribution of each object is estimated based on information about the partial occlusion and historical data. The examples mentioned above emphasise the potential of RL for addressing the grasping problem. However, when faced with the challenge of handling objects with varying shapes and stiffnesses, RL encounters several issues, such as complex network architectures, extensive training requirements, and sparse reward functions. Some of these training-related challenges can be mitigated by using the Sim2Real method, which entails intensive training in virtual environments followed by fine-tuning in the physical world [132]. However, achieving optimal performance in real-world settings is still a critical concern that necessitates further consideration.

IL provides a more straightforward approach for facilitating the acquisition of disassembly ability by robots than RL. The core idea revolves around enabling the robot to replicate the actions demonstrated by a human operator, thus acquiring human-like skills, commonly known as learning from demonstration (LfD) [133]. In an exploration of IL within the domain of disassembly, Vongbunyong et al. [134] developed a disassembly skill transfer platform. This platform uses visual sensors to capture the disassembly operations performed by an operator, subsequently enabling the robot to reproduce the disassembly process based on the recorded data. In the HRC-based LIB disassembly system developed by Gerbers et al. [20], disassembly actions were demonstrated by a human operator and executed by a robot via IL. Moreover, IL is widely employed in the field of grasping. Gao et al. [135] utilised a recurrent neural network (RNN) to model the trajectory data demonstrated by a human. They successfully generated smooth robot trajectories given knowledge of the grasping object's position and the robot's initial joint angle. Furthermore, their method proved to be robust against changes in the robot's initial joint angle. To adapt to the grasping of diverse objects, De Coninck et al. [136] implemented visual sensors at the robot actuator to capture images of objects during human demonstrations. These images were then fed into a CNN for learning, with the network outputting the optimal grasping point and angle for the object. Similarly, Zaatari et al. [137] employed a task-parameterised Gaussian mixture model (TP-GMM) to model demonstration trajectories encompassing various grasping directions. Additionally, they devised an RL algorithm based on the speeded-up robust figure (SURF) image processing algorithm, which effectively eliminated redundant grasping directions to assure accurate object recognition, localisation, and grasping path planning. In addition, the presence of parts with varying stiffness sizes within LIBs, such as softer cables and stiffer covers, presents a significant challenge in achieving successful grasping. The precise application of an appropriate grasping force plays a pivotal role in ensuring the success rate when handling these components. Lin et al. [138] employed a Gaussian mixture model (GMM) to effectively model force and position data acquired during human grasping of objects. Moreover, they utilised the Gaussian mixture regression (GMR) algorithm to simultaneously generate motion and force control trajectories for the robot. To enhance the adaptability of grasping objects with varying stiffness and size, Wang et al. [139] collected a comprehensive dataset comprising over 100 instances of robot demonstrations involving objects with different stiffness and size. This dataset included crucial information, such as grasping force and the bending angle of the gripper's finger joints. Subsequently, the researchers constructed three distinct depth networks, encompassing two different CNN network structures and a LSTM model, to effectively model the collected data. In this approach, real-time sensing data served as the network input, while the output dictated the driving speed of the finger joints, thereby enabling the proficient grasping of objects with varying characteristics.

IL presents notable advantages over RL, characterised by faster and simpler robot programming. However, the acquisition of complex disassembly operations, such as achieving a 6-DOF grasp, poses significant challenges when using IL. Furthermore, IL heavily relies on the quality and performance of demonstration data, rendering it less suitable for scenarios involving novices or noisy sensor data. To address these limitations, future research can focus on integrating IL with RL. This hybrid approach capitalises on the expertise of human demonstrators, enabling the utilisation of their valuable knowledge. Simultaneously, the robot can engage in autonomous exploration, enhancing knowledge generalisation and operational accuracy. Specific comparisons of the two methods are provided in Table 9.

5.3. HRC-based remote disassembly

HRC-based remote disassembly involves a human's remote instruction for a robot to accomplish disassembly tasks. This approach serves as an effective means of ensuring human safety during the disassembly process, particularly when faced with hazardous tasks related to LIBs,

Table 9
Two typical methods for obtaining robotic flexible disassembly ability.

Methods	Advantages	Disadvantages	Ref.
Reinforcement learning (RL)	• Automated data collection for learning purposes • Ability to learn complex disassembly operations	• Difficulty in setting the reward function • Requires large training amount • Slow learning efficiency	• Qu et al. [122] • Kristensen et al. [123] • Gualtieri et al. [127] • Hou et al. [128] • Wu et al. [129] • Hsiao et al. [130] • Pajarinen et al. [131]
Imitation learning (IL)	• No need to set the reward function in advance • Fast learning efficiency	• Poor ability to adapt and generalise • Heavily dependant on the quality of the demonstration	• Vongbunyong et al. [134] • Gao et al. [135] • De Coninck et al. [136] • El Zaatari et al. [137] • Lin et al. [138] • Wang et al. [139]

such as disassembling battery packs (which can lead to electrical leakage) and performing cutting operations (which can release toxic substances). Furthermore, the current technological limitations surrounding fully automated disassembly highlight the significance of HRC-based remote disassembly as a favourable solution. Currently, the solution has witnessed significant adoption in diverse domains, including underwater missions [140], space exploration [141], bomb disposal [142], and medical procedures [143]. These varied industrial applications serve as compelling examples of the solution's potential in managing hazardous manufacturing environments.

HRC-based remote disassembly can be achieved through three distinct levels of control, depending on how the robot is operated, and they are (1) direct control, (2) autonomous control, and (3) shared control. Direct control entails the operator exerting direct influence over every movement of the robot to successfully execute the task at hand. Odesanmi et al. [144] obtained real-time human motion data using a wearable device and simultaneously governed the articulations of a robotic manipulator in real time. Hathaway et al. [145] conducted a study on master-slave HRC-based remote systems for LIB disassembly. Specifically, two configurations were examined: a haptic device paired with a collaborative robot and a master-slave teleoperation system comprising two identical collaborative robots. The former demonstrated a higher overall success rate in completing the disassembly task, while the latter significantly reduced the task completion time for the entire disassembly process. Bellitti et al. [146] introduced a wireless wearable system capable of accurately tracking finger movements and recognising a diverse range of gestures (as shown in Fig. 9(a)). This technology offers the distinct advantage of being wire-free and allowing real-time control of the robot. While direct control represents the most efficient method of robot control, it is not immune to challenges, including communication delays and operational errors. Furthermore, achieving mastery in exerting full control over the robot is a demanding endeavour that necessitates extensive training and learning on the part of the operator. The second type of control is autonomous control, in which the robot possesses the capability to perform tasks independently without requiring continuous human guidance. In this mode, the robot receives instructions from the operator, but the actions taken by the robot are determined solely by its own decision-making processes. Muszynski et al. [147] developed a user interface that enables users to click on an object, prompting the robot to autonomously move to the appropriate position and grasp the selected object (as shown in Fig. 9(b)). However, it is important to note that most robots currently lack the level of intelligence necessary to autonomously complete tasks in unstructured and dynamic environments. Recognising the limitations of direct control and autonomous control, a middle ground referred to as shared control has emerged, enabling operators and robots to collaborate in task completion. For instance, in the case of controlling a dual robotic arm, Rakita et al. [148] advocated employing a sequence-to-sequence RNN to recognise various types of human movement and infer the optimal adaptable robot motion strategy. This augmentation assists the operator in executing tasks more seamlessly and efficiently (as shown in Fig. 9 (c)). Wang et al. [149] discovered that when employing a force feedback device to command a robotic arm, the device exhibited suboptimal responsiveness to the force exerted by a human operator. Consequently, a fuzzy variable conductance algorithm was designed to discern the user's movement intention and facilitate quick and precise responses. Moreover, to enhance the operator's understanding of the robot's operation and effectively manage uncertainties encountered in the field, Marino et al. [150] proposed harnessing AI techniques to process multiple sensor data, including vision, force, sound, etc., and introduced the implementation of a motion regulator capable of making subtle adjustments to the operator's guidance, ultimately enhancing operational accuracy. Based on the research presented, teleoperation emerges as a logical and promising approach for achieving safer and more efficient disassembly operations, particularly in the context of LIBs. Specific comparisons of these methods are provided in Table 10.

Furthermore, efforts between humans and robots to execute collaborative disassembly tasks in a shared workspace have been made. For instance, Zhou et al. [21] designed an HRC approach for screw removal from a battery's top cover. In this scenario, the robot makes decisions based on the human operator's actions by prioritising safety and efficiency. Huang et al. [151] implemented a HRC-based disassembly of press-fitted components, where the robot handles the shaft's grasp and the human engages in tapping the shaft. During the disassembly process, the robot adapts to the shaft's movements adeptly. Despite limited research specifically in the disassembly realm, extensive investigations in other domains have leveraged HRC for specialised tasks. Examples include: (i) the assembly of turbo gearboxes, where a human assembles bearings while a robot manages the transfer of bearings [152]; (ii) welding, where a human and a robot act together on the welding torch: the human controls the direction and speed while the robot suppresses sudden and abrupt motions [153]; (iii) screwing, where a human places screws into holes, and a robot takes charge of screwing operations [154]. The above approaches can be effectively applied in the disassembly process of EoL LIBs by approach repurposing and adapting.

5.4. Human safety during HRC-based disassembly operations

In HRC-enabled LIB disassembly scenarios, human safety is of utmost importance. Safety regulations that govern the interaction between industrial robots and humans are typically established based on recognised standards, such as ISO 10,218 [155–156]. To provide additional guidance and complement the ISO 10,218–1/2 standard, the technical specification ISO/TS 15,066 has been recently introduced [157]. This specification outlines four cooperation modes, namely, "safety-rated monitored stop (SRMS), "hand guided (HG), "speed and separation monitoring (SSM)," and "power and force limiting (PFL)". amongst these modes, it can be seen that the minimum distance between a human and a robot is an important safety index to avoid collision. In the SRMS operation mode, the robot comes to a stop or pauses its movement when the operator is detected within the robot workspace. On the other hand, in the SSM operation mode, the robot slows down or halts when the human approaches within the specified safety distance. Similarly, in the context of HRC-enabled disassembly, significant attention has been given to the determination of the minimum distance between a human and a robot. For instance, Xu et al. [67] investigated the impact of the minimum distance on the speed of the robot actuator while addressing the human-robot collaborative disassembly line balancing problem.

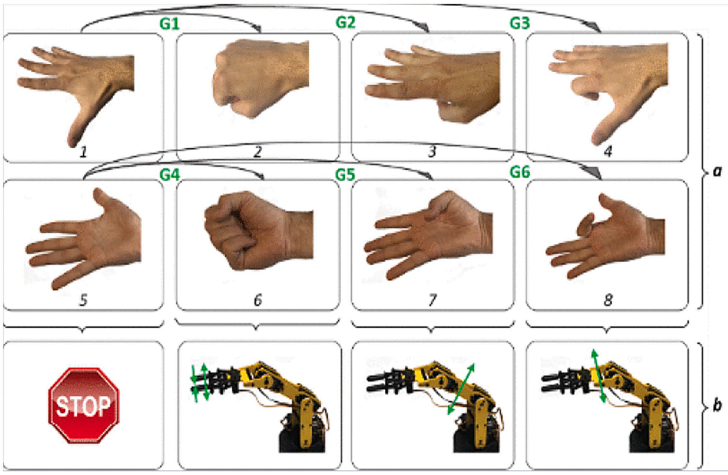

(a) Direct control of robots using gestures [146].

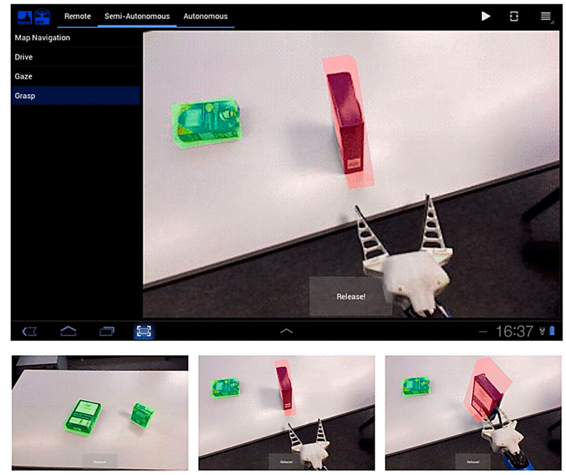

(b) An operator confirms the object to be grasped by tapping on the screen (the red object) [147].

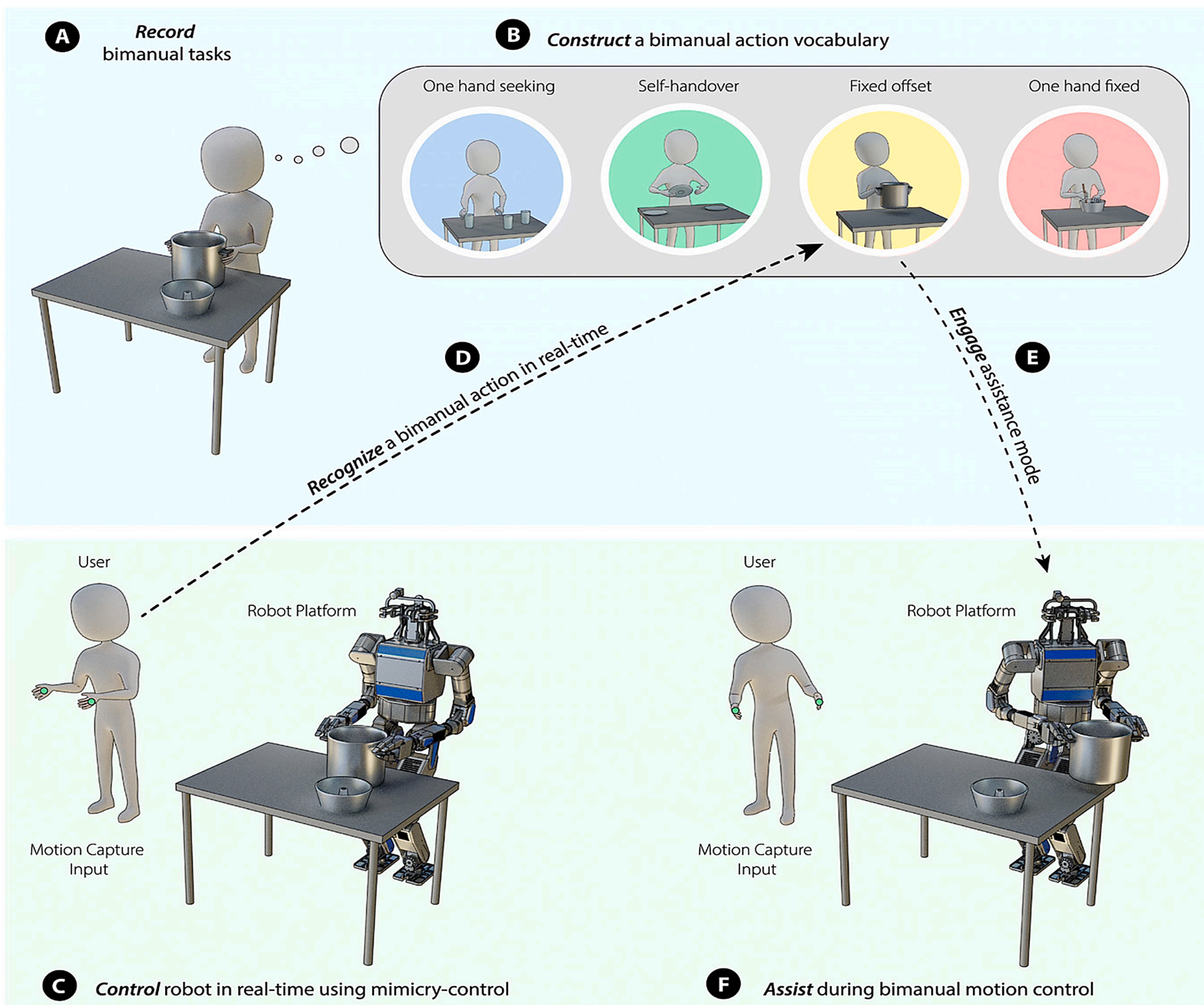

(c) An example of share control: robots help and support users to control movements [148].

Fig. 9. Examples to represent different robot control methods for HRC remote disassembly.

They established a function that relates the distance between the human and the robot to the speed of the robot, with closer distances resulting in slower speeds. Similarly, Lee et al. [158] examined whether the minimum distance between a human and a robot in a parallel-executed task falls below a safety threshold during the planning of an HRC-based disassembly sequence. If the distance is below the threshold, execution is prohibited. In another study, Lee et al. [96] utilised spatial location and distance between a human and a robot to predict the next

Table 10
Comparison of three typical methods for HRC-based remote disassembly.

Methods	Advantages	Disadvantages	Ref.
Direct control	• High safety • High efficiency • Simple control method	• Require low latency during signal transmission • Require operators to have high operational abilities	• Odesanmi et al. [144] • Hathaway et al. [145] • Bellitti et al. [146]
Autonomous control	• High safety • No need for operators to have high operational abilities • Cope with the actual situation during operation efficiently	• Require robots to have a high ability to adapt to dynamic and unstructured environments	• Muszynski et al. [147]
Shared control	• High safety • Fully leverage the respective advantages of human and robot • Able to complete tasks more accurately	• Require sufficient training • Limited generalisation capability	• Rakita et al. [148] • Wang et al. [149] • Marino et al. [150]

disassembly choice made by the human, thus supporting disassembly planning. Zhou et al. [21] considered the minimum distance between a human and a robot as an indicator of benefits in the development of a Stackelberg model. They employed this indicator to analyse the decision-making process of human-robot dismantling of screws. To summarise, ensuring a minimum distance between a human and a robot is crucial for establishing a safe HRC-enabled disassembly environment. Comparisons of several methods to calculate the minimum distance between a human and a robot are provided in Table 11.

To determine the minimum distance between a human and a robot, an accurate representation of their spatial poses is important. Common representations include bounding boxes, convex hulls, and geometric primitives. amongst these options, the bounding box method is the simplest approach [159,160]. It involves enclosing the point cloud of the human or robot within a minimal bounding box aligned with the coordinate axes (as depicted in Fig. 10(a)). The box is defined by two opposing corners, where one corner consists of the maximum coordinates of all the points in the point cloud, while the other corner consists of the minimum coordinates. By calculating the distance between the centres of each pair of bounding boxes, collision detection computations can be expedited. However, this method compromises accuracy because it does not take into account the specific contour information of the human and the robot. The convex hull approach offers improved accuracy over the bounding box method by leveraging the complete point cloud data. The main objective of the convex hull problem in geometry is to identify the smallest convex set that encompasses all the points, creating a polyhedron (as depicted in Fig. 10 (b)). Han et al. [161] demonstrated this approach by utilising an RGB-D sensor to capture a point cloud of the human arm. They then transformed the point cloud into a three-dimensional octree diagram and represented it as a convex hull for distance calculations, and the gilbert-johnson-keerthi (GJK) algorithm was employed to compute the distance. The GJK algorithm is a commonly used method for computing the distance between two convex hulls due to its efficiency and straightforward implementation. Similarly, Nikolakis et al. [162] employed a Kinect RGB-D sensor to capture the depth and skeletal data of the human body. They mapped the depth data onto the skeletal data to generate a point cloud representation of the body. Subsequently, a convex hull was constructed to envelop the body. This representation of the convex hull may reduce memory usage compared to the original point cloud data, but it introduces additional computation time. The geometric primitive approach, favoured for its computational efficiency, has become the prevalent method for representing humans and robots. This approach involves utilising a combination of standard geometric shapes (e.g., cylinders, spheres) to depict humans and robots (as depicted in Fig. 10(c)). For instance, Safeea et al. [163,164] employed three different sensors, including a magnetic tracking sensor, an inertial measurement unit (IMU), and a laser scanner, to track the positions of the human and the robot. The human and robot were represented using multiple capsule-shaped geometric primitives, with one capsule consisting of a cylinder and two hemispheres. The capsule shape was chosen due to its ability to capture the concave and convex nature resembling human limbs and robotic links. The human body was represented by five capsules, i.e., four to cover the right/left upper arm and forearm and a fifth to cover the torso up to the head. Three capsules were used to represent the collaborative robot. The minimum distance between these geometric primitives was calculated using a factorisation-based method, which offers a faster computational speed compared to the GJK algorithm. For a more accurate representation of the human body, Secil et al. [165,166] utilised six capsule-shaped geometric primitives to represent a human: one for the head, one for the torso, two for the upper arms, and two for the forearms. The GJK algorithm was then utilised to calculate the distance between the convex capsules. While the geometric primitive approach accelerates calculations, the computational cost increases as the number of capsules grows. Therefore, the number of capsules should be chosen judiciously to maintain computational efficiency.

Based on existing research, it is clear that safety in HRC-based disassembly environments necessitates distinct characterisation and sensing of various parts of the human body for collision detection and distance calculation. Moreover, the employment of geometric primitive representations has been shown to offer a rapid and efficient approach to computing minimum distances, particularly in real-time applications.

6. Discussion and future prospects

In this subsection, some potential and promising research directions are outlined and discussed (but are not limited to these directions).

Table 11
Typical methods to calculate the minimum distance between a human and a robot.

Methods	Advantages	Disadvantages	Ref. and methods of calculating distance
Bounding boxes	• Simple form • High efficiency	• Low accuracy	• Schmidt et al. [159]: the distance between the centres of each pair of bounding boxes • Mohammed et al. [160]: the distance between the centres of each pair of bounding boxes
Convex hulls	• High accuracy • Saves memory	• Long calculation time	• Han et al. [161]: GJK algorithm • Nikolakis et al. [162]: GJK algorithm
Geometric primitives	• High accuracy • High efficiency	• Difficulty in determining the appropriate number of geometric primitives	• Safeea et al. [163,164]: QR factorisation-based method • Secil et al. [165,166]: GJK algorithm

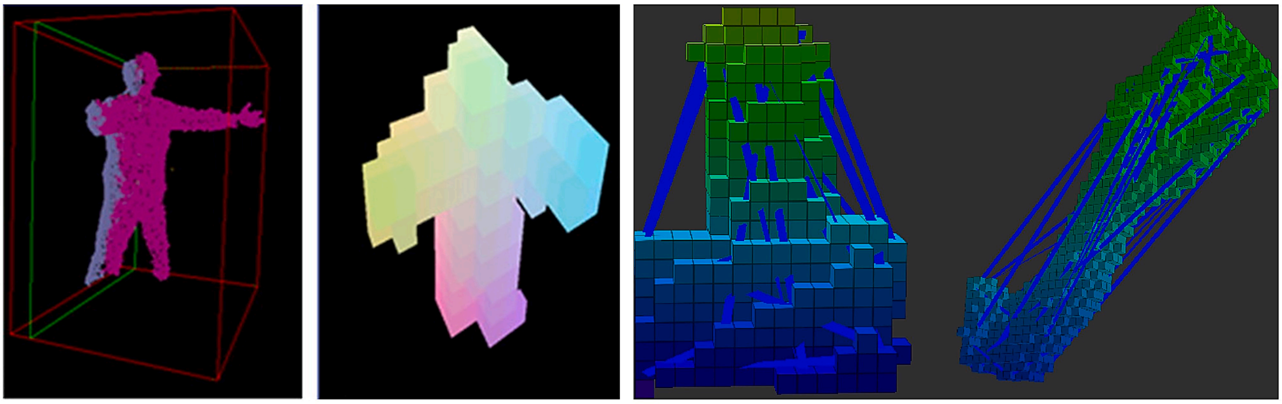

(a) Representing a point cloud of a human using a minimal bounding box [159].

(b) Constructing the convex hulls of non-convex models (a human arm and an obstacle) [161].

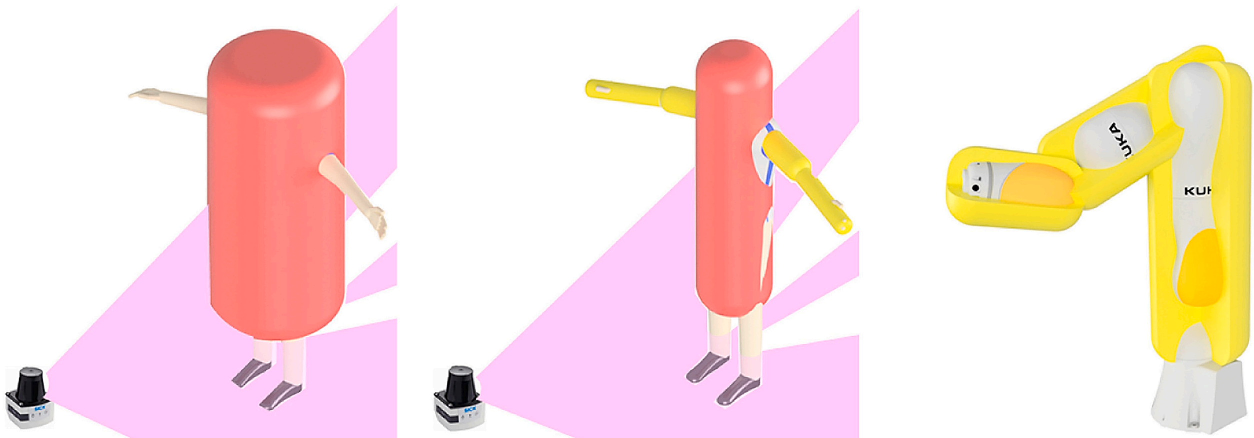

(c) A human represented by 1 capsule and 5 capsules, and a collaborative robot represented by 3 capsules [163].

Fig. 10. Several ways to represent the human and the robot.

The estimation of the remaining life and ageing conditions for LIBs is the most critical parameter to establish, screen, and sort LIBs. It is considered a fundamental step to determine their recycling and disassembly value. In recent years, data-driven intelligent estimation methods based on historical data have been developed [167,168]. However, it is a challenging task to carry out multiscale, accurate, and robust estimation, as the capacity attenuation, internal structures, and chemistry changes of spent LIBs are susceptible to many factors and utilisation conditions [17,24]. Without historical data, pack- and module-level assessments are highly complicated and equivalent to a black box due to the heterogeneous states of cells [17,24]. To close the gaps and better support recycling and disassembly decision-making, in-situ condition monitoring technologies should be integrated with intelligent battery management systems or cloud platforms to provide abundant data for rational decision-making in LIB recycling and disassembly.

As mentioned earlier, there are no international standards for EV LIB design. Thus, EoL LIB models are available in high varieties and various configurations with different joining technologies. This brings challenges to standardising HRC-based LIB disassembly processes. Meanwhile, recyclability, remanufacturability, and disassemblability philosophies have not been incorporated into LIB design, manufacturing, and assembly processes. There are numerically destructive, soft, and irregularly shaped parts and connectors in LIBs, such as nonstandard cables, fasteners, harnesses, and tabs, making the disassembly processes cumbersome and inefficient. Design for recyclability, remanufacturability, and disassemblability is highly imperative in next-generation LIB design.

The HRC-based LIB disassembly process is a complex, multifunctional, and dynamic endeavour. With humans being a crucial player during this process, it is imperative to establish a safe, comfortable, and convenient environment to facilitate humans during disassembly. Achieving such an environment may involve addressing the following requirements: (i) Build a multimodal sensing system. It is essential to implement a comprehensive sensing system, comprising industrial cameras, RGB-D cameras, thermal sensors, LIDAR sensors, robot-mounted eye-in-hand heat cameras, etc. How to effectively analyse and fuse the data from these sensors and feed the data back into the disassembly system is an important topic for further investigation; (ii) Ergonomic design. It can fine-tune the attention of humans or pre-processing information to support human decisions. Meanwhile, close collaboration between humans and robots can evoke changes in human psychology. It often stems from the fear of unknown factors, such as unpredictable robot behaviour or potential dangers in the LIB disassembly process. Addressing these concerns requires ergonomic design considerations. Possible solutions include designing HRC interfaces, developing cognitive adapters for decision-making, and improving information acquisition methods.

Safety issues during battery disassembly are foremost. Safety comes not only from batteries themselves, such as the avoidance of internal short circuits and thermal runaway, but also from the aspect of HRC. The safety strategies in HRC-based LIB disassembly should demonstrate varying degrees of applicability and adaptability in different disassembly scenarios. Research topics could include (i) the design of an evaluation measurement of an HRC-based disassembly task, which is used to categorise the task into subtasks based on the interaction and collaboration levels between robots and humans, and (ii) the design of multiple criteria (health and safety, throughput time, product yield, efficiency, etc.) optimisation algorithm for the entire lifecycle of disassembly tasks, which can switch different safety strategies and regulate robot behaviours to adapt to complex requirements in the subtasks [169].

Design new artificial intelligence algorithms to reuse or enhance demonstrations to facilitate HRC-based LIB disassembly. It is expensive to collect demonstrations to support robotic learning in various LIB disassembly scenarios. It is highly beneficial if the knowledge learned for one LIB disassembly scenario can be transferred to others, so time and cost can be significantly saved. Transfer learning, meta-learning, and incremental learning algorithms, which have been increasingly adopted for knowledge reuse, are promising artificial intelligence techniques to be leveraged. Regarding these algorithms, some open questions to be answered in future research include how to establish sensible learning algorithms to support efficient and effective knowledge sharing and increment and how to calibrate the knowledge from a prior task for new LIB disassembly scenarios.

Establishing a digital twin (DT) to support HRC-based LIB disassembly is pertinent. DT is a revolutionary technology that facilitates the seamless integration of the virtual and physical domains, thereby enhancing the simulation of complex industrial scenarios. Augmented Reality (AR) combined with DT can reduce the gap between the virtual and real worlds. Meanwhile, DT technology provides the same physical feedback as a real device. When applying HRC to new LIB disassembly, unforeseen risks may arise, while DT combined with AR provides a sensible solution. However, the integration of DT with HRC-based LIB disassembly encounters several challenges. First, existing DT systems lack a standardised framework model and architecture. When applied to LIB disassembly, bespoke models must be designed, incurring prohibitive costs [170]. Second, the success of DT relies heavily on the accuracy and real-time performance of data processing. However, current developments in the sensor technology cannot guarantee high-fidelity models in virtual environments. For instance, attempts at creating DT of a 3D printer show data processing with a 2–3 second delay [171]. This low latency, especially in complex disassembly environments, can significantly impact human safety. Finally, humans exhibit extremely high dynamic performance in HRC-based disassembly environments. Modelling a human operator and accurately replicating the exact digital version of the human is challenging. Though many studies attempt to predict human behaviour [172,173], such probabilistic results are still fraught with considerable uncertainty. An important future research topic is how to design sensible DT-based HRC solutions for LIB disassembly to validate the feasibility of disassembly operations, further improving safety and overall system performance.

7. Conclusions

Recycling EoL LIBs economically and sustainably has been a pressing topic in modern societies. Given the significance of EoL LIB disassembly in effectively supporting LIB recycling, it is highly valuable to summarise key technical enablers and the latest technical advances to shed light on how industries progress forward quickly. To provide systematic insights, in this survey, two pillars to uphold LIB disassembly, i.e., artificial intelligence and HRC technologies, are analysed. Furthermore, the related state-of-the-art LIB disassembly solutions are elaborated and discussed according to three major categories, namely, EoL LIB knowledge representation, disassembly planning, and disassembly operations. For each category, the major characteristics, pros and cons of methodologies are analysed and benchmarked in greater detail. Discussions on the current research gaps and forward-looking perspectives for the relevant developments are outlined. A pragmatic solution for EoL LIB disassembly needs to leverage the strengths of rapidly progressing AI, HRC, DT, etc. In future work, the related enabling technologies will be continuously explored. In particular, the learning, safety, and collaboration aspects of HRC to better support LIB disassembly will be the research focuses. Furthermore, data-driven monitoring and prognostic technologies to facilitate LIB disassembly decision-making will be investigated.

CRediT authorship contribution statement

Weidong Li: Writing – review & editing, Writing – original draft, Supervision, Project administration, Methodology, Investigation, Funding acquisition, Conceptualization. **Yiqun Peng:** Writing – original draft, Validation, Methodology, Investigation, Formal analysis, Data curation, Conceptualization. **Yu Zhu:** Writing – original draft, Visualization. **Duc Truong Pham:** Writing – review & editing, Supervision, Project administration, Funding acquisition, Conceptualization. **A.Y.C. Nee:** Writing – review & editing, Supervision, Funding acquisition, Conceptualization. **S.K. Ong:** Writing – review & editing, Methodology, Investigation, Formal analysis.

Declaration of competing interest

The authors claim that the manuscript is original and it is from the authors' own research. There are no conflict of interest or plagiarism issues in the manuscript.

Data availability

No data was used for the research described in the article.

Acknowledgement

This research was supported by several research, internationally collaborative, and overseas PhD scholarship projects of the National Natural Science Foundation of China (Project No. 51975444), the Ministry of Science and Technology of China (Project No. G2022013009), the Science and Technology Commission of Shanghai Municipality (Project No. 23010503700), the China Scholarship Council (Project No. 202206950015), and the Engineering and Physical Sciences Research Council, UK (Project No. EP/N018524/1).

References

[1] E. Kastanaki, A. Giannis, Dynamic estimation of end-of-life electric vehicle batteries in the EU-27 considering reuse, remanufacturing and recycling options, J. Clean. Prod 393 (2023) 136349.
[2] D. Kamath, S. Moore, R. Arsenault, A. Anctil, A system dynamics model for end-of-life management of electric vehicle batteries in the US: comparing the cost, carbon, and material requirements of remanufacturing and recycling, Resour. Conservat. Recycl. 196 (2023) 107061.
[3] A.M. Andwari, A. Pesiridis, S. Rajoo, R. Martinez-Rotas, Y. Esfahanian, A review of battery electric vehicle technology and readiness levels, Renew. Sustain. Energy Rev. 78 (2017) 414–430.
[4] S. Wu, N. Kaden, K. Droder, A systematic review on lithium-ion battery disassembly processes for efficient recycling, Batteries 9 (2023) 297.
[5] M.A. Hannan, M.M. Hoque, A. Hussain, Y. Yusof, P.J. Ker, State-of-the-art and energy management system of lithium-ion batteries in electric vehicle applications: issues and recommendations, IEEE. Access 6 (2018) 19362–19378.
[6] E. Gerlitz, M. Greifenstein, J. Hofmann, J. Fleischer, Analysis of the variety of lithium-ion battery modules and the challenges for an agile disassembly system, in: Proceedings of the 8th CRIP Global Web Conference - Flexible Mass Customisation, 2021, pp. 175–180.
[7] K. Richa, C.W. Babbitt, G. Gaustad, X. Wang, A future perspective on lithium-ion battery waste flows from electric vehicles, Res. Conservat. Recycl. 83 (2014) 63–76.
[8] W. Mrozik, M.A. Rajaeifar, O. Heidrich, P. Christensen, Environmental impacts, pollution sources and pathways of spent lithium-ion batteries, Energy Environ. Sci 14 (2021) 6099–6121.
[9] K. Edstrom. Battery 2030+ roadmap, 2021. https://battery2030.eu/wp-content/uploads/2021/08/c_860904-l_1-k_roadmap-27-march.pdf.
[10] L. Zhou, A. Garg, J. Zheng, L. Gao, K.Y. Oh, Battery pack recycling challenges for the year 2030: recommended solutions based on intelligent robotics for safe and efficient disassembly, residual energy detection, and secondary utilization, Energy Storage 3 (2021) e190.

[11] G. Harper, R. Sommerville, E. Kendrick, L. Driscoll, P. Slater, S.R.A. Walton, P. Christensen, O. Heidrich, S. Lambert, A. Abbott, K. Ryder, L. Linda Gaines, P. Anderson, Recycling lithium-ion batteries from electric vehicles, Nature 575 (2019) 75–86.
[12] H. Rallo, G. Benveniste, I. Gestoso, B. Amante, Economic analysis of the disassembling activities to the reuse of electric vehicles Li-ion batteries, Res. Conservat. Recycl. 159 (2020) 104785.
[13] M. Alfaro-Algaba, F. Javier Ramirez, Techno-economic and environmental disassembly planning of lithium-ion electric vehicle battery packs for remanufacturing, Res. Conservat. Recycl. 154 (2020) 104461.
[14] G. Tian, G. Yuan, A. Aleksandrov, T. Zhang, Z. Li, A.M. Fathollahi-Fard, M. Ivanov, Recycling of spent lithium-ion batteries: a comprehensive review for identification of main challenges and future research trends, Sustain. Energy Technol. Assess. 53 (2022) 102447.
[15] L. Qi, Y. Wang, L. Kong, M. Yi, J. Song, D. Hao, X. Zhou, Z. Zhang, J. Yan, Manufacturing processes and recycling technology of automotive lithium-ion battery: a review, J. Energy Stor. 67 (2023) 107533.
[16] D. Yu, Z. Huang, B. Makuza, X. Guo, Q. Tian, Pretreatment options for the recycling of spent lithium-ion batteries: a comprehensive review, Miner. Eng. 173 (2021) 107218.
[17] K. Meng, G. Xu, X. Peng, K. Youcef-Toumi, J. Li, Intelligent disassembly of electric-vehicle batteries: a forward-looking overview, Res. Conservat. Recycl. 182 (2022) 106207.
[18] J.F. Hellmuth, N.M. DiFilippo, M.K. Jounaneh, Assessment of the automation potential of electric vehicle battery disassembly, J. Manufact. Syst. 59 (2021) 398–412.
[19] S.E. Zaatari, M. Marei, W.D. Li, Z. Usman, Cobot programming for collaborative industrial tasks: an overview, Rob. Auton. Syst 116 (2019) 162–180.
[20] R. Gerbers, K. Wegener, F. Dietrich, K. Droder. Safe flexible and productive human-robot-collaboration for disassembly of lithium-ion batteries. Recycling of Lithium-Ion Batteries, Springer, 2018, pp. 99–126.
[21] Y. Zhou, Y.Q. Peng, W.D. Li, D.T. Pham, Stackelberg model-based human-robot collaboration in removing screws for product remanufacturing, Robot. Comput. Integr. Manuf 77 (2022) 102370.
[22] S.E. Zaatari, Y. Wang, Y. Hu, W.D. Li, An improved approach of task-parameterized learning from demonstrations for cobots in dynamic manufacturing, J. Intell. Manuf. 33 (2022) 1503–1519.
[23] C.W. Liu, J. Lin, H.B. Cao, Y. Zhang, Z. Sun, Recycling of spent lithium-ion batteries in view of lithium recovery: a critical review, J. Clean. Prod 228 (2019) 801–913.
[24] X. Lai, Y. Huang, C. Deng, H. Gu, X. Han, Y. Zheng, M. Ouyang, Sorting, regrouping, and echelon utilization of the large-scale retired lithium batteries: a critical review, Renew. Sustain. Energy Rev. 146 (2021) 111162.
[25] J. Neumann, M. Petranikova, M. Meeus, J.D. Gamarra, R. Younes, M. Winter, S. Nowak, Recycling of lithium-ion batteries - current state of the art, circular economy, and next generation recycling, Adv. Energy Mater 12 (2022) 2102917.
[26] D.L. Thompson, J.M. Hartley, S.M. Lambert, M. Shiref, G.D.J. Harper, E. Kendrick, P. Anderson, K.L. Ryder, L. Gaines, A.P. Abbott, The importance of design in lithium ion battery recycling – a critical review, Green. Chem. 22 (2020) 7585–7603.
[27] K. Wegener, W.H. Chen, F. Dietrich, K. Dröder, S. Kara, Robot assisted disassembly for the recycling of electric vehicle batteries, in: Proceedings of the 22nd CIRP Conference on Life Cycle Engineering 29, 2015, pp. 716–721.
[28] R. D`Souza, J. Patsavellas, K. Salonitis, Automated assembly of Li-ion vehicle batteries: a feasibility study, in: Proceedings of the 53rd CIRP Conference on Manufacturing Systems 93, 2020, pp. 131–136.
[29] I. Kay, S. Farhad, A. Mahajan, R. Esmaeeli, S.R. Hashemi, Robotic disassembly of electric vehicles' battery modules for recycling, Energies 15 (2022) 4856.
[30] M. Kaya, State-of-the-art lithium-ion battery recycling technologies, Circul. Eco. 1 (2022) 100015.
[31] J. Marshall, D. Gastol, R. Sommerville, B. Middleton, V. Goodship, E. Kendrick, Disassembly of Li ion cells – characterization and safety considerations of a recycling scheme, Metals. (Basel) 10 (2020) 773.
[32] A. Rastegarpanah, H.C. Gonzalez, R. Stolkin, Semi-autonomous behaviour tree-based framework for sorting electric vehicle batteries components, Robotics 10 (2021) 82.
[33] S. Rosenberg, S. Huster, S. Baazouzi, S. Glöser-Chahoud, A. Al Assadi, F. Schultmann, Field study and multimethod analysis of an EV battery system disassembly, Energies 15 (2022) 5324.
[34] M. Chu, W. Chen, Human-robot collaboration disassembly planning for end-of-life power batteries, J. Manufact. Syst. 69 (2023) 271–291.
[35] G. Yuan, X. Liu, C. Zhang, D.T. Pham, Z. Li, A new heuristic algorithm based on multi-criteria resilience assessment of human – robot collaboration disassembly for supporting spent lithium-ion battery recycling, Eng. Appl. Artif. Intell. 126 (2023) 106878.
[36] G. Foo, S. Kara, M. Pagnucco, Screw detection for disassembly of electronic waste using reasoning and re-training of a deep learning model, in: Proceedings of the 28th CIRP Conference on Life Cycle Engineering 98, 2021, pp. 666–671.
[37] Y. Zhang, X. Sun, K.J. Loh, W. Su, Z. Xue, X. Zhao, Autonomous bolt loosening detection using deep learning, Struct. Health Monit. 19 (1) (2020) 105–122.
[38] X. Li, M. Li, Y. Wu, D. Zhou, T. Liu, F. Hao, J. Yue, Q. Ma, Accurate screw detection method based on faster R-CNN and rotation edge similarity for automatic screw disassembly, Int. J. Comp. Integr. Manufact. 34 (11) (2021) 1177–1195.
[39] T. Bai, J. Yang, G. Xu, D. Yao, An optimized railway fastener detection method based on modified faster R-CNN, Measurement 182 (2021) 109742.
[40] I. Athanasiadis, A. Psaltis, A. Axenopoulos, P. Daras, Enhancing robot-assisted WEEE disassembly through optimizing automated detection of small components, Comp. Vision – ECCV. 2020. Workshops 16 (2020) 440–454.
[41] C. Su, J. Hu, P. Lou, Mask R-CNN based laptop parts detector for disassembly, in: Proceedings of the 5th International Conference on Machine Learning and Soft Computing, 2021, pp. 162–167.
[42] S. Mangold, C. Steiner, M. Friedmann, J. Fleischer, Vision-based screw head detection for automated disassembly for remanufacturing, in: Proceedings of the 29th CIRP Life Cycle Engineering Conference 105, 2022, pp. 1–6.
[43] M. Choux, E. Marti Bigorra, I. Tyapin, Task planner for robotic disassembly of electric vehicle battery pack, Metals. (Basel) 11 (3) (2021) 387.
[44] D.P. Brogan, N.M. DiFilippo, M.K. Jouaneh, Deep learning computer vision for robotic disassembly and servicing applications, Array 12 (2021) 100094.
[45] J. Chen, E. Bao, J. Pan, Classification and positioning of circuit board components based on improved YOLOv5, in: Proceedings of the 7th International Conference on Intelligent, Interactive Systems and Applications 208, 2022, pp. 613–626.
[46] S. Zheng, F. Lan, L. Baronti, D.T. Pham, M. Castellani, Automatic identification of mechanical parts for robotic disassembly using the PointNet deep neural network, Int. J. Manufact. Res. 17 (1) (2022) 1–21.
[47] H. Brådland, M. Choux, L.R. Cenkeramaddi, Point cloud instance segmentation for automatic electric vehicle battery disassembly, in: Proceedings of the International Conference on Intelligent Technologies and Applications 1616, 2021, pp. 247–258.
[48] C. Wu, X. Bi, J. Pfrommer, A. Cebulla, S. Mangold, J. Beyerer, Sim2real transfer learning for point cloud segmentation: an industrial application case on autonomous disassembly, in: Proceedings of the IEEE/CVF Winter Conference on Applications of Computer Vision, 2023, pp. 4531–4540.
[49] J. Redmon, S. Divvala, R. Girshick, A. Farhadi, You only look once: unified, real-time object detection, in: Proceedings of the IEEE Conference on Computer Vision and Pattern Recognition, 2016, pp. 779–788.
[50] R. Girshick, J. Donahue, T. Darrell, J. Malik, Rich feature hierarchies for accurate object detection and semantic segmentation, in: Proceedings of the IEEE Conference on Computer Vision and Pattern Recognition, 2014, pp. 580–587.
[51] M. Zorn, C. Ionescu, D. Klohs, K. Zähl, N. Kisseler, A. Daldrup, S. Hams, Y. Zheng, C. Offermanns, S. Flamme, C. Henke, A. Kampker, B. Friedrich, An approach for automated disassembly of lithium-ion battery packs and high-quality recycling using computer vision, labeling, and material characterization, Recycling 7 (4) (2022) 48.
[52] M.F. Adesso, R. Hegewald, N. Wolpert, E. Schömer, B. Maier, B.A. Epple, Automatic classification and disassembly of fasteners in industrial 3D CAD-Scenarios, in: 2022 International Conference on Robotics and Automation, 2022, pp. 9874–9880.
[53] M.T. Bilal, I. Tyapin, M.M.H. Choux, Fusion of multiview images for EV battery disassembly, in: 2023 11th International Conference on Control, Mechatronics and Automation, 2023, pp. 19–24.
[54] C.R. Qi, H. Su, K. Mo, L.J. Guibas, Pointnet: deep learning on point sets for 3d classification and segmentation, in: Proceedings of the IEEE Conference on Computer Vision and Pattern Recognition, 2017, pp. 652–660.
[55] G. Tian, M. Zhou, P. Li, Disassembly sequence planning considering fuzzy component quality and varying operational cost, IEEE. Transact. Automat. Sci. Engin. 15 (2) (2017) 748–760.
[56] M.L. Bentaha, A. Dolgui, O. Battaïa, R.J. Riggs, J. Hu, Profit-oriented partial disassembly line design: dealing with hazardous parts and task processing times uncertainty, Int. J. Producti. Res. 56 (24) (2018) 7220–7242.
[57] Y. Ren, L. Meng, C. Zhang, F. Zhao, U. Saif, A. Huang, G.P. Mendis, J. W. Sutherland, An efficient metaheuristics for a sequence-dependent disassembly planning, J. Clean. Prod. 245 (2020) 118644.
[58] C. Xu, H. Wei, X. Guo, S. Liu, L. Qi, Z. Zhao, Human-robot collaboration multi-objective disassembly line balancing subject to task failure via multi-objective artificial bee colony algorithm, IFAC-PapersOnLine 53 (5) (2020) 1–6.
[59] Y. Liu, M. Zhou, X. Guo, An improved Q-learning algorithm for human-robot collaboration two-sided disassembly line balancing problems, in: Proceedings of the IEEE International Conference on Systems, Man, and Cybernetics, 2022, pp. 568–573.
[60] X. Guo, S. Liu, M. Zhou, G. Tian, Disassembly sequence optimization for large-scale products with multiresource constraints using scatter search and Petri nets, IEEE. Trans. Cybern. 46 (11) (2015) 2435–2446.
[61] X. Guo, M. Zhou, S. Liu, L. Qi, Multiresource-constrained selective disassembly with maximal profit and minimal energy consumption, IEEE. Transact. Automat. Sci. Engin. 18 (2) (2020) 804–816.
[62] Y. Ren, H. Guo, Y. Li, J. Li, L. Meng, A self-adaptive learning approach for uncertain disassembly planning based on extended petri net, IEEE Transact. Indust. Informat. (2023) (Online).
[63] Y. Tang, M. Zhou, M. Gao, Fuzzy-Petri-net-based disassembly planning considering human factors, Syst. Humans 36 (4) (2006) 718–726.
[64] H. Mao, Z. Liu, C. Qiu, Adaptive disassembly sequence planning for VR maintenance training via deep reinforcement learning, Int. J. Adv. Manufact. Technol. (2021) 1–10.
[65] S. Parsa, M. Saadat, Human-robot collaboration disassembly planning for end-of-life product disassembly process, Robot. Comput. Integr. Manuf 71 (2021) 102170.
[66] W. Xu, Q. Tang, J. Liu, Z. Liu, Z. Zhou, D.T. Pham, Disassembly sequence planning using discrete Bees algorithm for human-robot collaboration in remanufacturing, Robot. Comput. Integr. Manuf. 62 (2020) 101860.

[67] W. Xu, J. Cui, B. Liu, J. Liu, B. Yao, Z. Zhou, Human-robot collaborative disassembly line balancing considering the safe strategy in remanufacturing, J. Clean. Prod. 324 (2021) 129158.
[68] T. Wu, Z. Zhang, T. Yin, Y. Zhang, Multi-objective optimisation for cell-level disassembly of waste power battery modules in human-machine hybrid mode, Waste Manage 144 (2022) 513–526.
[69] X. Liu, G. Peng, X. Liu, Y. Hou, Disassembly sequence planning approach for product virtual maintenance based on improved max–min ant system, Int. J. Adv. Manufac. Technol. 59 (5) (2012) 829–839.
[70] J. Xiao, N. Anwer, W.D. Li, B. Eynard, C. Zheng, Dynamic Bayesian network-based disassembly sequencing optimization for electric vehicle battery, CIRP. J. Manufac. Sci. Technol. 38 (2022) 824–835.
[71] S.S. Min, X.J. Zhu, X. Zhu, Mechanical product disassembly and/or graph construction, in: Proceedings of the International Conference on Measuring Technology and Mechatronics Automation 2, 2010, pp. 627–631.
[72] J.C. Chen, Y.Y. Chen, T.L. Chen, Y.C. Yang, An adaptive genetic algorithm-based and AND/OR graph approach for the disassembly line balancing problem, Engin. Optimizat. 54 (9) (2022) 1583–1599.
[73] L. Jin, X. Zhang, Y. Fang, D.T. Pham, Transfer learning-assisted evolutionary dynamic optimisation for dynamic human-robot collaborative disassembly line balancing, App. Sci. 12 (21) (2022) 11008.
[74] K. Wegener, S. Andrew, A. Raatz, K. Dröder, C. Herrmann, Disassembly of electric vehicle batteries using the example of the Audi Q5 hybrid system, in: Proceedings of the Conference on Assembly Technologies and Systems 23, 2014, pp. 155–160.
[75] K. Xia, L. Gao, W.D. Li, L. Wang, K.M. Chao, A Q-learning based selective disassembly planning service in the cloud based remanufacturing system for WEEE, in: Proceedings of the ASME 2014 International Manufacturing Science and Engineering Conference 45806, 2014. V001T04A012.
[76] D.E. Grochowski, Y. Tang, A machine learning approach for optimal disassembly planning, Int. J. Comp. Integ. Manufact. 22 (4) (2009) 374–383.
[77] Y. Tang, Learning-based disassembly process planner for uncertainty management, Syst. Humans 39 (1) (2008) 134–143.
[78] K. Xia, L. Gao, L. Wang, W.D. Li, K.M. Chao, A simplified teaching-learning-based optimization algorithm for disassembly sequence planning, in: Proceedings of the 2013 IEEE 10th International Conference on e-Business Engineering, 2013, pp. 393–398.
[79] C. Pornsing, A. Watanasungsuit, Discrete particle swarm optimization for disassembly sequence planning, in: Proceedings of the 2014 IEEE International Conference on Management of Innovation and Technology, 2014, pp. 480–485.
[80] Y. Laili, F. Ye, Y. Wang, L. Zhang, Interference probability matrix for disassembly sequence planning under uncertain interference, J. Manufact. Syst. 60 (2021) 214–225.
[81] F. Ye, J. Perrett, L. Zhang, Y. Laili, Y. Wang, A self-evolving system for robotic disassembly sequence planning under uncertain interference conditions, Robot. Comput. Integr. Manuf 78 (2022) 102392.
[82] X. Zhao, C. Li, Y. Tang, J. Cui, Reinforcement learning-based selective disassembly sequence planning for the end-of-life products with structure uncertainty, IEEE. Robot. Automat. Letters 6 (4) (2021) 7807–7814.
[83] A. ElSayed, E. Kongar, S.M. Gupta, T. Sobh, An online genetic algorithm for automated disassembly sequence generation, in: International Design Engineering Technical Conferences and Computers and Information in Engineering Conference 54808, 2011, pp. 657–664.
[84] Y. Laili, F. Tao, D.T. Pham, Y. Wang, L. Zhang, Robotic disassembly re-planning using a two-pointer detection strategy and a super-fast bees algorithm, Robot. Comput. Integr. Manuf 59 (2019) 130–142.
[85] H. Cheng, W. Xu, Q. Ai, Q. Liu, Z. Zhou, D.T. Pham, Manufacturing capability assessment for human-robot collaborative disassembly based on multi-data fusion, Proc. Manufactur. 10 (2017) 26–36.
[86] K. Li, Q. Liu, W. Xu, J. Liu, Z. Zhou, H. Feng, Sequence planning considering human fatigue for human-robot collaboration in disassembly, in: Proceedings of the 11th CIRP Conference on Industrial Product-Service Systems 83, 2019, pp. 95–104.
[87] B. Liu, W. Xu, J. Liu, B. Yao, Z. Zhou, D.T. Pham, Human-robot collaboration for disassembly line balancing problem in remanufacturing, in: Proceedings of the International Manufacturing Science and Engineering Conference 58745, 2019. V001T02A037.
[88] L. Guo, Z. Zhang, X. Zhang, Human-robot collaborative partial destruction disassembly sequence planning method for end-of-life product driven by multi-failures, Adv. Engin.. Informat. 55 (2023) 101821.
[89] Y. Liu, Z. Jiang, C. Ke, A task allocation method in human-robot collaboration (HRC) for the disassembly of automotive traction batteries, in: Proceedings of the 2022 International Conference on Cyber-Physical Social Intelligence (ICCSI), 2022, pp. 332–337.
[90] P.K.R. Maddikunta, Q.V. Pham, B. Prabadevi, N. Deepa, K. Dev, T.R. Gadekallu, R. Ruby, M. Liyanage, Industry 5.0: a survey on enabling technologies and potential applications, J. Indust. Informat. Integrat., 26 (2022) 100257.
[91] Y. Chen, Y. Luo, M.O. Yerebakan, S. Xia, S. Behdad, B. Hu, Human workload and ergonomics during human-robot collaborative electronic waste disassembly, in: Proceedings of the 2022 IEEE 3rd International Conference on Human-Machine Systems (ICHMS), 2022, pp. 1–6.
[92] Z. Zhou, J. Liu, D.T. Pham, W. Xu, F.J. Ramirez, C. Ji, Q. Liu, Disassembly sequence planning: recent developments and future trends, in: Proceedings of the Institution of Mechanical Engineers, Part B: Journal of Engineering Manufacture 233, 2019, pp. 1450–1471.
[93] S.K. Ong, M.M.L. Chang, A.Y.C. Nee, Product disassembly sequence planning: state-of-the-art, challenges, opportunities and future directions, Int. J. Product. Res. 59 (11) (2021) 3493–3508.
[94] M. Weyrich, N. Natkunarajah, Conception of an automated plant for the disassembly of lithium-ion batteries, in: Proceedings of the 6th International Conference on Life Cycle Management, Gothenburg, Sweden, 2013.
[95] L. Lander, C. Tagnon, V. Nguyen-Tien, E. Kendrick, R. Elliott, A.P. Abbott, J. S. Edge, G.J. Offer, Breaking it down: a techno-economic assessment of the pact of battery pack design on disassembly cost, Appl. Energy 331 (2023) 120437.
[96] M.L. Lee, W. Liu, S. Behdad, X. Liang, M. Zheng, Robot-assisted disassembly sequence planning with real-time human motion prediction, IEEE Transact. Sys. Man,. Cybern.:. Sys. 53 (1) (2022) 438–450.
[97] H.Y. Liao, Y. Chen, B. Hu, S. Behdad, Optimization-based disassembly sequence planning under uncertainty for human-robot collaboration, J. Mech. Des. 145 (2) (2023) 022001.
[98] C. Xiang, P. Liu, J. Guo, J. Wang, S. Qin, L. Qi, J. Zhao, Multi-neighborhood parallel greedy search algorithm for human-robot collaborative multi-product hybrid disassembly line balancing problem, in: Proceedings of the 2022 IEEE International Conference on Systems, Man, and Cybernetics (SMC), 2022, pp. 866–871.
[99] S. Behdad, D. Thurston, Disassembly and reassembly sequence planning tradeoffs under uncertainty for product maintenance, J. Mech. Des. 134 (4) (2012) 041011.
[100] S. Vongbunyong, S. Kara, M. Pagnucco, Learning and revision in cognitive robotics disassembly automation, Robot. Comput. Integr. Manuf. 34 (2015) 79–94.
[101] J. Yu, H. Zhang, Z. Jiang, W. Yan, Y. Wang, Q. Zhou, Disassembly task planning for end-of-life automotive traction batteries based on ontology and partial destructive rules, J. Manufact. Syst. 62 (2022) 347–366.
[102] E. Villagrossi, T. Dinon, Robotics for electric vehicles battery packs disassembly towards sustainable remanufacturing, J. Remanufact. 13 (3) (2023) 355–379.
[103] J. Schäfer, R. Singer, J. Hofmann, J. Fleischer, Challenges and solutions of automated disassembly and condition-based remanufacturing of lithium-ion battery modules for a circular economy, Proc. Manufact. 43 (2020) 614–619.
[104] L. Li, P. Zheng, T. Yang, R. Sturges, M.W. Ellis, Z. Li, Disassembly automation for recycling end-of-life lithium-ion pouch cells, JOM 71 (2019) 4457–4464.
[105] Y. Lu, M. Maftouni, T. Yang, P. Zheng, D. Young, Z.J. Kong, Z. Li, A novel disassembly process of end-of-life lithium-ion batteries enhanced by online sensing and machine learning techniques, J. Intell. Manuf. 34 (5) (2023) 2463–2475.
[106] S. Hjorth, D. Chrysostomou, Human-robot collaboration in industrial environments: a literature review on non-destructive disassembly, Robot. Comput. Integr. Manuf 73 (2022) 102208.
[107] D. Mironov, M. Altamirano, H. Zabihifar, A. Liviniuk, V. Liviniuk, D. Tsetserukou, Haptics of screwing and unscrewing for its application in smart factories for disassembly, in: Proceedings of the International Conference on Human Haptic Sensing and Touch Enabled Computer Applications, 2018, pp. 428–439.
[108] Y. Zhang, H. Lu, D.T. Pham, Y. Wang, M. Qu, J. Lim, S. Su, Peg-hole disassembly using active compliance, R. Soc. Open. Sci 6 (8) (2019) 190476.
[109] X.L. Guo, B.H. Sun, Assembly and disassembly mechanics of a spherical snap fit, Theor. App. Mech. Letters 13 (1) (2023) 100403.
[110] R. Li, D.T. Pham, J. Huang, Y. Tan, M. Qu, Y. Wang, M. Kerin, K. Jiang, S. Su, C. Ji, Q. Liu, Z. Zhou, Unfastening of hexagonal headed screws by a collaborative robot, IEEE Transact. Automat. Sci. Engin. 99 (2020) 1–14.
[111] J. Huang, D.T. Pham, R. Li, K. Jiang, D. Lyu, C. Ji, Strategies for dealing with problems in robotised unscrewing operations, Smart Technol. Prec. Assem. (2021) 93–107.
[112] F. Wang, S. Zhang, S. Hao, H. Shu, The nondestructive disassembly method of interference fit of sleeve-base structure in the case of cooling excitation, in: Proceedings of the International Conference on Sustainable Design and Manufacturing, 2019, pp. 455–469.
[113] S. Su, D.T. Pham, C. Ji, Y. Wang, J. Huang, W. Zhou, H. Wang, Design of a compliant device for peg-hole separation in robotic disassembly, Int. J. Adv. Manufact. Technol. (2022) 1–9.
[114] W. Liu, J.K. Mills, MEMS remote centre of compliance design, in: Proceedings of the 2006 International Conference on Mechatronics and Automation, 2006, pp. 118–123.
[115] P. Schumacher, M. Jouaneh, A force sensing tool for disassembly operations, Robot. Comput. Integr. Manuf. 30 (2) (2014) 206–217.
[116] P. Schumacher, M. Jouaneh, A system for automated disassembly of snap-fit covers, Int. J. Adv. Manufact. Technol. 69 (9) (2013) 2055–2069.
[117] J. Carrell, D. Tate, S. Wang, H.C. Zhang, Shape memory polymer snap-fits for active disassembly, J. Clean. Prod. 19 (17–18) 2066–2074.
[118] A. Billard, D. Kragic, Trends and challenges in robot manipulation, Science 364 (6446) (2019) eaat8414.
[119] M.T. Mason, Toward robotic manipulation, Ann. Rev. Control, Robot. Autonom. Sys. 1 (2018) 1–28.
[120] A.I. Károly, P. Galambos, J. Kuti, I.J. Rudas, Deep learning in robotics: survey on model structures and training strategies, Systems 51 (1) (2020) 266–279.
[121] O. Kroemer, S. Niekum, G. Konidaris, A review of robot learning for manipulation: challenges, representations, and algorithms, J. Mach. Learn. Res. 22 (1) (2021) 1395–1476.
[122] M. Qu, Y. Wang, D.T. Pham, Robotic disassembly task training and skill transfer using reinforcement learning, IEEE Transact. Indust. Informat. 19 (11) (2023) 10934–10943.

[123] C.B. Kristensen, F.A. Sørensen, H.B. Nielsen, M.S. Andersen, S.P. Bendtsen, S. Bøgh, Towards a robot simulation framework for e-waste disassembly using reinforcement learning, in: Procedia Manufacturing 38, 2019, pp. 225–232.
[124] M. Lauri, D. Hsu, J. Pajarinen, Partially observable markov decision processes in robotics: a survey, IEEE Transac. Robot. 39 (1) (2022) 21–40.
[125] S. Vongbunyong, W.H. Chen, S. Vongbunyong, W.H. Chen, Disassembly Automation, Springer, 2015, pp. 25–54.
[126] M.Q. Mohammed, K.L. Chung, C.S. Chyi, Review of deep reinforcement learning-based object grasping: techniques, open challenges, and recommendations, IEEE Access 8 (2020) 178450–178481.
[127] M. Gualtieri, R. Platt, Learning 6-dof grasping and pick-place using attention focus, in: Proceedings of 2nd Conference on Robot Learning, 2018, pp. 477–486.
[128] Y. Hou, J. Li, Learning 6-DoF grasping with dual-agent deep reinforcement learning, Rob. Auton. Syst 166 (2023) 104451.
[129] B. Wu, I. Akinola, J. Varley, P. Allen, Mat: multi-fingered adaptive tactile grasping via deep reinforcement learning, in: Proceedings of the 3rd Conference on Robot Learning, 2019 arXiv: 1909.04787.
[130] K. Hsiao, L.P. Kaelbling, T. Lozano-Perez, Grasping pomdps, in: Proceedings of the 2007 IEEE International Conference on Robotics and Automation, 2007, pp. 4685–4692.
[131] J. Pajarinen, V. Kyrki, Robotic manipulation of multiple objects as a POMDP, Artif. Intell 247 (2017) 213–228.
[132] W. Zhao, J.P. Queralta, T. Westerlund, Sim-to-real transfer in deep reinforcement learning for robotics: a survey, in: Proceedings of the 2020 IEEE Symposium Series on Computational Intelligence (SSCI), 2020, pp. 737–744.
[133] H. Ravichandar, A.S. Polydoros, S. Chernova, A. Billard, Recent advances in robot learning from demonstration, Annual Rev. Control, Robot., Autonom. Syst 3 (2020) 297–330.
[134] S. Vongbunyong, P. Vongseela, J. Sreerattana-aporn, A process demonstration platform for product disassembly skills transfer, in: Proceedings of the 24th CIRP Conference on Life Cycle Engineering 61, 2017, pp. 281–286.
[135] Z. Gao, N.Y. Chong, Efficient robotic grasp learning by demonstration, in: RITA 2018: Proceedings of the 6th International Conference on Robot Intelligence Technology and Applications, 2020, pp. 87–99.
[136] E. De Coninck, T. Verbelen, P. Van Molle, P. Simoens, B. Dhoedt, Learning robots to grasp by demonstration, Rob. Auton. Syst 127 (2020) 103474.
[137] S.E. Zaatari, Y. Wang, W.D. Li, Y. Peng, iTP-LfD: improved task parametrised learning from demonstration for adaptive path generation of cobot, Robot. Comput. Integr. Manuf 69 (2021) 102109.
[138] Y. Lin, S. Ren, M. Clevenger, Y. Sun, Learning grasping force from demonstration, in: Proceedings of the 2012 IEEE International Conference on Robotics and Automation, 2012, pp. 1526–1531.
[139] S. Wang, W. Hu, L. Sun, X. Wang, Z. Li, Learning adaptive grasping from human demonstrations, IEEE/ASME Transac. Mechatr 27 (5) (2022) 3865–3873.
[140] G.G. Muscolo, S. Marcheschi, M. Fontana, M. Bergamasco, Dynamics modeling of human–machine control interface for underwater teleoperation, Robotica 39 (4) (2021) 618–632.
[141] H. Chen, P. Huang, Z. Liu, Mode switching-based symmetric predictive control mechanism for networked teleoperation space robot system, IEEE/ASME Transac. Mechatr 24 (6) (2019) 2706–2717.
[142] A. Ibarra, A. Cóndor, P. Martínez, E. Tipán, Control reengineering used for rehabilitation of andros remotec bomb disposal robot, in: Proceedings of the 2020 IEEE ANDESCON, 2020, pp. 1–6.
[143] H. Peng, X. Yang, Y.H. Su, B. Hannaford, Real-time data driven precision estimator for raven-ii surgical robot end effector position, in: Proceedings of the 2020 IEEE International Conference on Robotics and Automation (ICRA), 2020, pp. 350–356.
[144] G.A. Odesanmi, Q. Wang, J. Mai, Skill learning framework for human-robot interaction and manipulation tasks, Robot. Comput. Integr. Manuf 79 (2023) 102444.
[145] J. Hathaway, A. Shaarawy, C. Akdeniz, A. Aflakian, R. Stolkin, A. Rastegarpanah, Towards reuse and recycling of lithium-ion batteries: tele-robotics for disassembly of electric vehicle batteries, Front. Robot. AI 10 (2023) 1179296.
[146] P. Bellitti, A. De Angelis, M. Dionigi, E. Sardini, M. Serpelloni, A. Moschitta, P. Carbone, A wearable and wirelessly powered system for multiple finger tracking, IEEE Trans. Instrum. Meas 69 (5) (2020) 2542–2551.
[147] S. Muszynski, J. Stückler, S. Behnke, Adjustable autonomy for mobile teleoperation of personal service robots, in: Proceedings of the 2012 IEEE RO-MAN: The 21st IEEE International Symposium on Robot and Human Interactive Communication, 2012, pp. 933–940.
[148] D. Rakita, B. Mutlu, M. Gleicher, L.M. Hiatt, Shared control-based bimanual robot manipulation, Sci. Robot.. 4 (30) (2019) eaaw0955.
[149] Y.H. Wang, G.Y. Liu, G. Huang, Y. Wang, Variable admittance force feedback device and its human-robot interaction stability, Robot. Comput. Integr. Manuf 82 (2023) 102537.
[150] D.L. Marino, J. Grandio, C.S. Wickramasinghe, K. Schroeder, K. Bourne, A. V. Filippas, M. Manic, AI augmentation for trustworthy AI: augmented robot teleoperation, in: Proceedings of the 2020 13th International Conference on Human System Interaction (HSI), 2020, pp. 155–161.
[151] J. Huang, D.T. Pham, Y. Wang, M. Qu, C. Ji, S. Su, W. Xu, Q. Liu, Z. Zhou, A case study in human-robot collaboration in the disassembly of press-fitted components, in: Proceedings of the Institution of Mechanical Engineers, Part B: Journal of Engineering Manufacture 234, 2020, pp. 654–664.
[152] Y. Zhang, K. Ding, J. Hui, S. Liu, W. Guo, L. Wang, Skeleton-RGB integrated highly similar human action prediction in human-robot collaborative assembly, Robot. Comput. Integr. Manuf 86 (2024) 102659.
[153] M.S. Erden, B. Marić, Assisting manual welding with robot, Robot. Comput. Integr. Manuf 27 (4) (2011) 818–828.
[154] S. Nikolaidis, P. Lasota, R. Ramakrishnan, J. Shah, Improved human-robot team performance through cross-training, an approach inspired by human team training practices, Int. J. Rob. Res 34 (14) (2015) 1711–1730.
[155] International Standard Organisation, ISO 10218-1: 2011. Robots and Robotic devices—Safety Requirements For Industrial Robots-Part 1: Robots, International Standard Organisation, 2011.
[156] International Standard Organisation, ISO 10218-2: 2011. Robots and Robotic Devices—Safety Requirements For Industrial Robots-Part 2: Robot systems and Integration, International Standard Organisation, 2011.
[157] International Standard Organisation, ISO/TS 15066: 2016. Robots and Robotic Devices-Collaborative Robot, International Organisation for Standardisation, 2016.
[158] M.L. Lee, S. Behdad, X. Lian, M. Zheng, Task allocation and planning for product disassembly with human-robot collaboration, Robot. Comput. Integr. Manuf 76 (2022) 102306.
[159] B. Schmidt, L. Wang, Depth camera based collision avoidance via active robot control, J. Manufac. Syst 33 (4) (2014) 711–718.
[160] A. Mohammed, B. Schmidt, L. Wang, Active collision avoidance for human-robot collaboration driven by vision sensors, Int. J. Comp. Integr. Manufac 30 (9) (2017) 970–980.
[161] D. Han, H. Nie, J. Chen, M. Chen, Dynamic obstacle avoidance for manipulators using distance calculation and discrete detection, Robot. Comput. Integr. Manuf 49 (2018) 98–104.
[162] N. Nikolakis, V. Maratos, S. Makris, A cyber physical system (CPS) approach for safe human-robot collaboration in a shared workplace, Robot. Comput. Integr. Manuf 56 (2019) 233–243.
[163] M. Safeea, P. Neto, Minimum distance calculation using laser scanner and IMUs for safe human-robot interaction, Robot. Comput. Integr. Manuf 58 (2019) 33–42.
[164] M. Safeea, N. Mendes, P. Neto, Minimum distance calculation for safe human robot interaction, Proced. Manufac 11 (2017) 99–106.
[165] S. Secil, M. Ozkan, Minimum distance calculation using skeletal tracking for safe human-robot interaction, Robot. Comput. Integr. Manuf 73 (2022) 102253.
[166] S. Secil, M. Ozkan, A collision-free path planning method for industrial robot manipulators considering safe human-robot interaction, Intell. Service Robot.ics (2023) 1–37.
[167] X. Hu, F. Feng, K. Liu, L. Zhang, J. Xie, B. Liu, State estimation for advanced battery management: key challenging and future trends, Renew. Sustain. Energy Rev 114 (2019) 109334.
[168] M. Ng, J. Zhao, Q. Yan, G.J. Conduit, Z.W. She, Predicting the state of charge and health of batteries using data-driven machine learning, Nat. Mach. Intellig 2 (3) (2020) 161–170.
[169] W.D. Li, Y.D. Hu, Y. Zhou, D.T. Pham, Safe human-robot collaboration for industrial settings: a survey, J. Intell. Manuf (2023) accepted and online.
[170] P. Aivaliotis, K. Georgoulias, K. Alexopoulos, Using digital twin for maintenance applications in manufacturing: state of the Art and Gap analysis, in: 2019 IEEE International Conference on Engineering, Technology and Innovation (ICE/ITMC), 2019, pp. 1–5.
[171] P. Zheng, A.S. Sivabalan, A generic tri-model-based approach for product-level digital twin development in a smart manufacturing environment, Robot. Comput. Integr. Manuf 64 (2020) 101958.
[172] B. Yao, B. Yang, W. Xu, Z. Ji, Z. Zhou, L. Wang, Virtual data generation for human intention prediction based on digital modeling of human-robot collaboration, Robot. Comput. Integr. Manuf 87 (2024) 102714.
[173] J. Zhang, P. Wang, R.X. Gao, Hybrid machine learning for human action recognition and prediction in assembly, Robot. Comput. Integr. Manuf 72 (2021) 102184.